PACIFIC DECADAL VARIABILITY: STRUCTURE AND MECHANISMS

A scholarly paper submitted to the Department of Atmospheric and Oceanic Science of the University of Maryland, College Park in partial fulfillment of the requirements for the degree of Master of Science
2006

Bin Guan
Advisor: Professor Sumant Nigam

Abstract

Unlike El Niño/Southern Oscillation (ENSO), spatiotemporal structures of Pacific decadal variability (PDV) remains to be robustly defined, due, in part, to the relative short lengths of available data sets; subsurface observations relevant to PDV are especially few and sparse. The resulting ambiguity in PDV characterization, among others, leads to difficulties in analyzing the mechanisms operative in PDV.

The first part of the proposed work is to improve characterization of PDV structures and evolution. The primary analysis will be based on rotated extended empirical orthogonal function (EOF) of a variety of ocean-atmosphere data sets; the analysis will be designed such that all major modes of Pacific low-frequency variability (e.g., biennial variability, ENSO, PDV, etc.) are extracted in a single step. Features of the analysis include using of unfiltered data, a Pan-Pacific analysis domain and inclusion of all four seasons in the analysis; all for the purpose of a consistent way of modal extraction. The results from rotated extended EOF will be corroborated with those from other analysis (e.g., canonical correlation analysis). Stability/physicality of the extracted modes is one major concern, which will be assessed via sensitivity tests and/or correlations with non-physical data, say, biological productivity. Expectation is to provide a robust and physically meaningful PDV modal extraction, which proves to be promising according to a pilot analysis of a century-long sea surface temperature (SST) data set.

The second part of the work involves exploration of PDV mechanisms, via data analysis and diagnostic modeling. Lead/lag relationships between key oceanic and atmospheric variables will be analyzed in observations and in coupled simulations, in context of PDV; of interest is SST anomalies in the Pacific Tropics and midlatitudes that are connected via atmospheric and/or oceanic "bridges". Diagnostic modeling is proposed to help understand the influence of SST anomalies on local and remote near-surface circulation and fluxes at different stages of PDV evolution. The role of upper ocean, on the other hand, will be investigated by analyzing the PDV-covarying heat content. Volumetric heat balance in the upper ocean will be evaluated in an effort to understand the relative importance of surface heat fluxes and subsurface processes in PDV context.

Table of Contents

List of Figures

List of Tables

Chapter 1

Introduction

The Pacific ocean is home to several types of recurrent modes of low-frequency variability, from interannual to interdecadal. Unlike El Niño/Southern Oscillation (ENSO) which dominates interannual SST variability in the equatorial central/eastern Pacific and is now relatively well defined as a phenomenon involving air-sea interactions, the Pacific decadal/interdecadal variability (PDV) turns out to have more complicated structures in the Pacific Tropics as well as in midlatitudes, and, due in part to the relatively short lengths of observational data sets, remains to be robustly characterized.

The significance of PDV has been recognized only in the last decade. Longer than those associated with ENSO, climate variations on decadal/multidecadal time scales are of greater economic and societal importance since potential episodes may span a significant portion of human life, and of other species as well. The PDV has received considerable scientific attention after mid-1990's when climate and fisheries have appeared linked in the North Pacific (e.g., Mantua et al. 1997; Barlow et al. 2001; Chavez et al. 2003). The PDV has considerable significance also in the context of potential global warming. Given its time scale, it may not always be immediately clear if/how the effects of the PDV (which is natural) differ from those of global warming. This is even more true in context of variations/changes in the marine ecosystems since observations are few and sparse. It is of interest to note that the current status of our understanding of the PDV is not without some parallels to that of ENSO in the 1980's, suggesting that targeted observations, among others, may be crucial in advancing understanding, modeling and prediction of PDV.

The empirical orthogonal function (EOF) method has, among others, been common to researchers in modal decomposition in context of Pacific decadal variability (PDV), due, by definition, to its ability to extract the leading modes that most effectively explain the covariance structure of the data being analyzed. In these EOF-based analyses (and many other eigenanalyses), the existence of one or more decadal modes in the Pacific SST variability that are essentially different/independent from ENSO is beyond doubt. The modal structures and interpretations thereof however exhibit considerable diversity among different analyses, examples being Deser and Blackmon (1995), Zhang et al. (1996), Zhang et al. (1997), Mantua et al. (1997), Nakamura et al. (1997), Barlow et al. (2001) and Wu et al. (2003). These analyses, though all EOF-based, often differ in the way the covariance matrix was constructed. Particularly, pre-filtering of the physical fields being analyzed is not uncommon, and the frequency bands used for filtering are often analysis-dependent. Rotation of eigenvectors—

a technique intended to simplify the structure and hence physical interpretation of the EOF modes—probably makes another major difference in modal extraction. Selection of analysis domain and periods, among others, could also have contributed to the issue to considerable extent, especially considering the inherent inefficiency of regular EOF analysis in some particular cases (see more discussions in Chapter 3).

The first part of the proposed work is motivated by the historical ambiguity in the characterization of Pacific decadal variability, and the potential to improve by advanced statistical techniques. In general, previous studies have identified at least two structurally different SST modes on decadal time scales: a "Pan-Pacific" mode, with SST spatial patterns reminiscent of those in the mature phase of El Niño, and a "North Pacific" mode which, unlike ENSO or the Pan-Pacific mode, only have signatures in the central North Pacific. In general, observational studies fall into two groups in terms of the number of PDV patterns they are proposing: the unimodal group and the bimodal group. It is of interest to note that even if within the same group, modal extractions and interpretations often differ to considerable extent.

Even more challenging than PDV characterization is the tracing of PDV origins and evolution mechanisms. Due to scarcity of observations, existing PDV theories are largely developed from modeling studies. The inability of models to realistically simulate the ENSO *cycle* (e.g., amplitudes, aperiodicity, seasonal phase-locking, etc.) is however suggestive of their limited potential in PDV simulation, currently; things are rapidly improving, though.

Theories indicate that the Pacific midlatitudes may be a key region of decadal variability (Latif and Barnett 1994)—one that is connected to the Tropics through both the atmosphere (Pierce et al. 2000; Vimont et al. 2003) and ocean (Liu et al. 1994). In contrast, Jacobs et al. (1994) posit the Pacific Tropics to be the source of decadal variability; with propagation to the midlatitudes via the ocean. Another influential theory, proposed by Gu and Philander (1997), suggests that the Tropics affects the midlatitudes via the atmosphere, while the return influence is through the ocean. The second part of the proposed work, in context of the various PDV theories, seeks to better understand the atmospheric/oceanic linkages between decadal variations in the Tropics and midlatitudes. Particularly, impacts of SST variations on local and, via the atmosphere, on remote near-surface circulation and fluxes will be dynamically diagnosed at different stages of PDV evolution. Ocean heat content will be analyzed to understand the oceanic linkage, on the other hand.

In Chapter 2, recent studies on PDV are briefly reviewed. A description of the proposed work, including data and methodology, is given in Chapter 3. A pilot analysis of Pacific low-frequency variability—based on rotated extended EOF of a century-long SST data set—are described in Section 4. Chapter 5 gives the work schedule. The formulation of the rotated extended EOF is given in Appendix A.

Chapter 2

Pacific Decadal Variability: A Brief Review

Due to its important relevance to regional and perhaps remote climate, PDV has been receiving intensive attentions in the recent decade, with advances made in many aspects. However, due to its complicated spatial and temporal structure(s), our current understanding of PDV is still far from comparable to ENSO. This chapter reviews what we know about PDV and what we do not.

2.1 Overview

Foreseen by some earlier researchers, the significance of PDV yet only became recognized by the scientific community in the past decade. Studies on spatial and temporal structures of PDV, as well as its impact on local and remote climate abounded in mid-1990's. Due to the limitation of data lengths/coverage and performance of numerical models, the study and understanding of PDV is now still an ongoing process, with unknows and uncertainties in various aspects. It is interesting to note that our current status of understanding on PDV is not with some parallels to that of ENSO in the 1980's.

Decadal to multidecadal variations in Northern Hemisphere ocean and atmosphere were shown to be significant by observational studies as early as in 1980's. Specifically, a "regime shift" was revealed to have taken place around 1976–77. For example, Folland and Parker (1989) found decadal mean hemispheric surface temperature anomalies were larger in magnitude and more coherent during 1977–86 than in other decades (beginning in 1947). Trenberth (1990) showed SLP was significantly lower in the North Pacific during the winter months of 1977–88 than those of 1924–76. Also, he found that variations in North Pacific SLP during 1947–87 were highly correlated with the PNA (Wallace and Gutzler 1981), a preferred mode of atmospheric variability in boreal winters, suggesting the former to be a surface signature of the PNA teleconnection patterns. The findings in SST and SLP variations were cross-validated among independent studies. The associated changes in wind stress curl and hence the gyral circulation were implied. A physical picture were therefore emerging for the North Pacific ocean and atmosphere: a deepened Aleutian low brings about enhanced westerlies to the south, cooling the SST via increased air-sea heat flux, oceanic mixing and

thermal advection. Increased SST gradients further enhance the original westerly anomalies, forming a positive feedback. In the meanwhile, southerly (northerly) anomalies to the east (west) of the Aleutian low would bring warmer (colder) air to the west coast of North America (central North Pacific), leading to positive (negative) SST anomalies. Aside from the physical consistency, this picture however could not answer questions as where does the change come from in the first place, and what sets up the time scale for the change to take place.

Earlier studies had speculated that decadal variability in the North Pacific could be caused by internal atmospheric variability, unstable air-sea interactions and/or tropical-extratropical teleconnections. Data and model unavailability seemed to have been a major impediment to a clearer description. Indeed, the longer time scale and probably broader spatial signatures made it a more demanding topic than did ENSO. Without the benefit of hindsight, it was also then hard to say whether the "regime shift" around 1976–77 is a unique event or merely part of some ocean/atmosphere variability that may be more oscillatory in nature. Two types of point of view, as a result, coexisted in literature (probably up to present), each supported by early observational and modeling studies.

With state-of-the-art coupled ocean-atmosphere models, Latif and Barnett (1994, 1996) explored dynamically the causes and predictability of decadal variability in the North Pacific, and developed a consistent physical picture to explain the phase change and time scale for one mode of PDV. Specifically, the study emphasized on midlatitude air-sea interactions in forcing PDV, which differed from some earlier studies. For example, Nitta and Yamada (1989) examined the relationship between the warming trend of tropical SSTs and Northern Hemisphere circulation, and attributed PDV to SST anomalies in equatorial central/western Pacific. Trenberth and Hurrell (1994) suggested that though midlatitude air-sea interactions may be important, the origins of PDV shall be find in the equatorial Pacific. Also, numerical simulations by Lau and Nath (1994) showed that SST anomalies associated with ENSO could induce large-scale circulation anomalies in the extratropical North Pacific whereas *in situ* SST anomalies in the extratropical North Pacific cannot.

In the meanwhile, studies attempted to investigate PDV in the context of interannual ENSO variability. Unlike PDV, ENSO had by then been recognized as a well-defined phenomenon due to tropical air-sea interactions, the impacts of which may extend well away from tropical origins via ocean/atmosphere teleconnections. Indeed, some studies had been arguing that tropical SST anomalies may induce extratropical SST anomalies via the PNA teleconnection pattern in the atmosphere. It was then common sense to ask whether PDV is related to ENSO, or more specifically, whether PDV is a linear response to ENSO. The answer of Zhang et al. (1996) was "no". Basically, they compared signatures of PDV ("North Pacific mode" in the ocean and PNA-like mode in the atmosphere) between total fields of SST/500-hPa geopotential height and those with ENSO linearly removed, the results showing that the removal of ENSO did not affect the modal structure of the above modes, nor did it affect the covariability of extratropical ocean and atmosphere. Probably with the benefit of rotation, the EOF-based characterization revealed a more coherent PDV structure (even if without temporal filtering), one with opposite polarities of SST anomalies in central North Pacific and along the west coast of North America, while virtually no signatures in the tropics. That PDV is not linearly related to ENSO warranted further seek of *in situ* origins of the former.

Subsequent study of Zhang et al. (1997) further demonstrated the existence of a decadal

mode in the tropical-extratropical Pacific. Unlike in Zhang et al. (1996), the SST spatial pattern identified therein was not confined to the central North Pacific. Rather, it was more like the SST pattern associated with ENSO, except that SST anomalies was less equatorially confined in the tropical eastern Pacific, and larger in magnitude in extratropical North Pacific than in tropical Pacific (hence the term "ENSO-like" interdecadal variability). The study showed that the 1976–77 regime shift is not a unique event, which has a counterpart of opposite polarity during the 1940's. That decadal variability and interannual variability shares similar spatial structures in ocean and atmosphere is much intriguing.

Broadly in accordance with Zhang et al. (1997), Mantua et al. (1997) emphasized the coherence (and perhaps the oscillatory nature, hence the term "Pacific decadal oscillation" or PDO) of PDV, one existed across a variety of climatological and ecological records and throughout the 20^{th} century. Based on some PDO index (which is now widely used in climate research) and other indices defined therein, three regime shifts in the 20^{th} century were proposed to have taken place in 1925, 1947 and 1977, respectively; virtually the same dates for regime shifts were proposed in an independent study by Minobe (1997). According to the latter study, regime shifts were present not only in central/eastern North Pacific and western North America, but also in the Indian Ocean-maritime continent region and Japan. Particularly, spatial and temporal patterns of temperatures reconstructed from tree ring widths in the western North America agreed well with instrumental data with respect to regime shifts in the 20^{th} century. It was then shown that regime shifts on interdecadal time scales could actually be dated back to the end of 18^{th} century with the reconstructed data. Noteworthy was the term "50–70 year climatic oscillation" used by Minobe (1997) perhaps to emphasize the pentadecadal time scale, which physically may or may not be akin to the bidecadal mode proposed by Latif and Barnett (1994), for example. The relationship between these two types of modes with obviously different time scales was investigated in a subsequent study by Minobe (1999). It was found that both were needed to explain the regime shifts, with the pentadecadal mode setting up the time scale for climate regimes, while the bidecadal mode—via synchronization with the former—realizing rapid transitions across opposite regimes.

In the meanwhile, interests arose as whether/how the tropical and extratropical Pacific interact on interannual to interdecadal time scales, especially given the somewhat similar spatial structures of ENSO and PDV in ocean/atmosphere as was demonstrated by Zhang et al. (1997), for example. In view of the large inter-event variability (hence less predictability) of ENSO teleconnections in North America, Gershunov and Barnett (1998) investigated the modulation of the former by PDV and concluded that ENSO teleconnections (in SLP and precipitation) were more strong and coherent when PDV (in their words "North Pacific Oscillation", or "NPO") was in a favorable phase. In other words, PDV might give rise to decadal climate variability in North America given PDV itself is somehow predictable. Barnett et al. (1999a,b) found that decadal variability in North Pacific has at least two simultaneously occurring components: one stochastically forced (with no preferred time scale), driven by the atmosphere (amplified by air-sea interaction, though), while the other deterministically forced (of period 20 years), driven by ocean-atmosphere coupling, and it is the stochastically forced component that modulates tropical ENSO variability via atmospheric teleconnections.

2.2 PDV structure

Part of the confusion about PDV comes from the somewhat ambiguous and perhaps contradictory descriptions of its spatiotemporal structures especially in the ocean. Indeed, a variety of names (e.g., regime shifts, ENSO-like interdecadal variability, PDO, NPO, etc.) have been used in literature to refer to PDV, which by itself is an evidence of lack of consensus. That PDV may consists of more than one mode further complexes the problem. This section reviews vis-à-vis various modes of PDV identified by previous studies and differences thereof (to the extent they are comparable) so as to better understand the complexity of PDV, if not PDV itself.

2.2.1 Temporal characteristics

PDV was often referred to as regime shift(s) in early studies perhaps due to the relative shortness of any data sets to uncover/ascertain its recurrence. Of special relevance is the frequently mentioned regime shift occurred around 1976–77, which, with the benefit of hindsight, can be viewed merely as a manifestation of one or more occurring modes on decadal time scales except perhaps with larger magnitudes and coherence than other episodes on record. Various aspects of the 1976–77 regime shift were investigated by early observational (e.g., Nitta and Yamada 1989) and modeling (e.g., Miller et al. 1994) studies. Related to this shift is negative (positive) SST anomalies on the order of 1°C in central and western North Pacific (Alaska), and deepened wintertime Aleutian low by several millibars, as described by Trenberth (1990). Of interest is the seasonal phase-locking, i.e., greater changes tend to be observed during the winter (a parallel to ENSO). Besides the one occurred around 1976–77, several other regime shifts were reported by later studies (e.g., Mantua et al. 1997; Minobe 1997). Over the time, regime shifts turned out to be more like manifestations of recurrent mode(s) rather than unrelated events.

2.2.2 Spatial patterns

Among others, EOF have been a common tool in previous studies for PDV modal extraction. In addition to selection of analysis domain and period, studies often differ in the details the data are prepared. For example, some analyses used only the winter season, while others used all seasons. Some used prefiltered data, some not. Rotation of eigenvectors was also used in some studies for the purpose of simplified modal structures.

Despite the varied data treatment, the PDV mode(s) thereby identified generally fall into two types[1]: a "Pan-Pacific" mode[2], with SST spatial patterns reminiscent of those in the mature phase of El Niño[3], and a "North Pacific" mode which, unlike ENSO or the Pan-Pacific mode, only have signatures in the central North Pacific. The extent to which the Pan-Pacific mode resembles the ENSO mode in structure differ among studies and analyses.

[1]Note individual analyses may have only identified or addressed one of the two modes.

[2]The name used here is for the purpose of consistent terminology, which does not necessarily reflect the actual name used by original authors.

[3]One distinguished feature is the out-of-phase relationship between SST anomalies in equatorial central/eastern Pacific and extratropical North Pacific.

For example, in Zhang et al. (1997, their Fig. 3, lowest panel) the Pan-Pacific mode [extracted from unrotated EOF of 6-yr low-pass filtered COADS[4] SST (Fletcher et al. 1983) in the Pacific domain[5]] is a whole lot like ENSO except greater SST anomalies are found in the extratropical North Pacific rather than equatorial central/eastern Pacific. On the other hand, in Barlow et al. (2001, their Fig. 2b) the same mode [extracted from rotated EOF of unfiltered UWM/COADS[6] SST (da Silva et al. 1994) in the Pacific north of 20°S] has less signal in the equatorial eastern Pacific than in ENSO [and also less signal in the North Pacific than in Zhang et al. (1997)]. Using unrotated EOF of unfiltered *wintertime* COADS SST in the Pacific north of 20°S, Deser and Blackmon (1995, their Fig. 1b) identified a North Pacific mode that is linearly independent of ENSO. Interestingly, using unrotated EOF of unfiltered HSSTD[7] (Folland and Parker 1990, 1995) in the Pacific north of 20°N, Mantua et al. (1997, their Fig. 2a) identified a mode—in their terminology the "Pacific Decadal Oscillation (PDO)"—that is spatially reminiscent of Barlow et al. (2001)'s North Pacific mode but temporally akin to their Pan-Pacific mode. Unlike Mantua et al. (1997), Nakamura et al. (1997, their Fig. 2a,b) reported two decadal modes based on unrotated EOF of unfiltered *wintertime* COADS SST in the North Pacific (20–50°N, 150°E–140°W). Of interest in their study is that even if the EOF analysis was performed in a restricted domain in the North Pacific, regressions of SST anomalies onto the principal components suggest that one of the two modes has considerable connections to the Tropics/subtropics. That PDV may consists of two co-existent modes—one essentially restricted to the Pacific midlatitudes (North Pacific mode), while the other having comparable signatures in the Tropics and subtropics (Pan-Pacific mode)—surfaces more in later studies using rotated EOF analysis, for example, Barlow et al. (2001, their Fig. 2b,c) with unfiltered UWM/COADS SST and Wu et al. (2003, their Fig. 1a,b) with 8-yr low-pass filtered Kaplan et al. (1998)'s SST.

2.3 PDV mechanisms

As seen from the previous section, PDV may consists of more than one mode that differ from one another spatially and/or temporally. Specifically, PDV may have signatures in both tropics and extratropics. Different (but not necessarily exclusive) mechanisms have been proposed to explain one or more of the modes. This section reviews various processes that may contribute to PDV in different manners.

2.3.1 Atmospheric variability

It has been found that without interactions with the ocean, internal atmospheric variability by itself can force a PDV mode, except perhaps with smaller amplitude. Support of this type of argument dates back to Hasselmann (1976) and Frankignoul and Hasselmann (1977). Due to its large thermal inertia and heat content, ocean may synthesize the effects of stochastic (spectrally "white") processes in the atmosphere and manifest them as a "reddened" spectrum

[4]Comprehensive Ocean-Atmosphere Data Set.
[5]They somehow did not explicit the exact domain used in the EOF analysis.
[6]University of Wisconsin-Milwaukee version of COADS.
[7]U.K. Meteorology Office (UKMO)'s historical SST data set.

that has more power on the lower frequency band. Indeed, the power spectrum of SST can—to the first order of approximation—be regarded as "red" in both observations and modeling studies. In the case of PDV, internal atmospheric variability may come from the PNA teleconnection patterns of which central North Pacific is a center of action. Aside from the geographic preference and probable seasonal phase-locking (since PNA dominants in boreal winters), PDV may be essentially unpredictable if the above mechanism accounts for all or majority of PDV.

2.3.2 Oceanic variability

Due to data sparseness, the majority of PDV studies lacks an insight of subsurface variables and dynamics therein. Conceivably, SST variations in the Pacific midlatitudes could be generated by wind-induced surface forcing as well as by subsurface dynamics. Indeed, simulations with ocean GCMs showed that significant decadal variability in SST could be found in the Kuroshio Extension which is a "window" (opens only in winter) area of surface-subsurface interactions (Xie et al. 2000). Using the production of a simple ocean data assimilation (Carton et al. 2000b,a), Tomita et al. (2002) diagnosed the relative importance of surface forcing and subsurface geostrophic advection in generating decadal SST variations; the latter was found to contribute significantly in the Kuroshio-Oyashio Extension. Recent study by Hosoda et al. (2004) reassured the importance of subsurface dynamics in PDV simulation. That subsurface plays an important role in PDV suggests the latter to be potentially predictable as subsurface observations and simulations advance.

2.3.3 Coupled dynamics

Probably the most influential coupled scenario of PDV is the one described by Latif and Barnett (1994, 1996), and later Barnett et al. (1999a,b). In this scenario, the subtropical gyre and the Aleutian low were found to be the most important components in the ocean and in the atmosphere, respectively. As surface heat fluxes and wind-induced oceanic mixing act to reinforce the initial SST anomalies, it is the transient response of the ocean to variations in the wind stress curl that either strengthens or weakens the gyral circulation such that the signs of SST anomalies are to reversed; the coupled system hence oscillates (see Latif and Barnett 1994 for a detailed description). Predictability could therefore be inferred since the decadal time scale is determined by the memory of the ocean in the coupled system.

2.4 Summary

The studies reviewed have all suggested the existence of PDV in the extratropical and perhaps tropical Pacific. Local atmospheric variability, air-sea interactions, as well as ocean/atmosphere teleconnections may all be needed to explain the significance of PDV. Particularly, PDV may be forced by internal atmospheric variability alone, but owes the preferred decadal time scale to ocean-atmosphere coupling. As seen, PDV may consists of more than one mode which may involve with rather different mechanisms and have different

impacts locally and/or remotely. Regime shifts (e.g. the one occurred around 1976–77) are likely to be realizations of one or more of these modes.

Our understanding of PDV is at a somewhat primitive stage, which involves with considerable amount of confusions and unknowns. Of particular priority shall be a robust and improved extraction and description of PDV modal structure(s) with advanced mathematical tools and hopefully newly available data sets (particularly subsurface observations and data assimilation products). Subject to this, it is also of special interest to re-examine the tropical-extratropical connections in view of ENSO-PDV superposition in literature.

Chapter 3

Proposed Work

3.1 Hypothesis

Our understanding of the PDV is still at a primitive stage, in a sense. Much progress, nonetheless, has been made toward a clear description of PDV structures and the underlying processes in the ocean and atmosphere. The working hypothesis is that PDV may involve co-existent modes (may or may not be independent) in different sections of the Pacific basin that have different structures and/or mechanisms. It is believed that carefully designed statistical analysis (to be detailed later) can help to robustly identify such modes, which will then provide the basis for observational and modeling studies that will be needed to clarify the ocean-atmosphere processes and mechanisms operative in PDV.

3.2 Objectives

The overall issue reviewed in Chapter 2 begs answers to the following questions: Does PDV indeed involve more than one *physical* mode? Is PDV of tropical or extratropical origin? Without time filtering, is PDV structurally separable from interannual ENSO variability? Is there a consistent way to extract *all* the physically significant low-frequency modes (e.g., biennial, ENSO, PDV, etc.) in the Pacific SST variability? How does PDV evolve in time and how does it affect local and remote climate? The current study aims to address all the above questions, of which the priority is to robustly extract and describe the PDV modal structures and their evolution. The overall objectives of my research are therefore proposed as follows:

- Improve the characterization of PDV structures using advanced statistical techniques; importance will be placed on the stability/sensitivity of such characterization.
- Advance understanding of the PDV mechanisms and its impacts on local and remote climate. Tropical-extratropical connections will be investigated to better understand the relationships between ENSO and PDV.

The primary analysis will be based on the so-called "rotated extended EOF" of seasonally resolved, unfiltered SST anomalies in a Pan-Pacific domain during the period of 1900–2002.

The analysis will be designed in such a way that all the low-frequency modes are extracted in a single step, and that modal extractions are stable and physically meaningful.

3.3 Data

The primary data set to be used is UKMO[1]'s HadISST[2] 1.1 SST, which is globally available on 1°×1° grids and spans the period of 1870–current (in this work, 2002) at monthly intervals. HadISST temperatures were constructed using a reduced-space optimal interpolation followed by quality-controlled gridded observations onto the reconstruction (Rayner et al. 2003). Because of its relatively long record, continuity and statistical homogeneity, HadISST is well suited to be used in the statistical analysis for PDV characterization. Another oceanic data set to be used is SIO[3]'s ocean heat content. The data set covers all longitudes within 60°S–60°Nwith a 5° Long×2° Lat resolution, and is currently available for the period of 1955–2003 at monthly intervals. It is noted that NODC[4] has also produced an ocean heat content data set (Levitus et al. 2005). The data set covers all the ocean basins with a 1°×1° resolution, which however is only available on a yearly basis, currently[5], for the period of 1955 to 2003. Still in search of is a reasonably long data set of air-sea heat flux; with UWM/COADS (da Silva et al. 1994) being a potential candidate. For the atmosphere, the NCEP/NCAR reanalysis (Kalnay et al. 1996) will be used. In addition to observed and reanalyzed data, the output of IPCC[6]'s 20^{th} century climate simulations will be used to assess PDV representation in coupled models.

For EOF analysis, the SST data at each grid cell are weighted by the square root of the cosine of the latitude. The seasonal cycle, determined by long-term mean of each season, is removed. The data are then normalized by domain-averaged standard deviation (rather than by standard deviation of individual grid cells). Normalized this way locations with greater variability will have more weight in the analysis, as they should indeed. Caution is used not to impose any *a priori* periodicity (e.g., time filtering) on the data.

In view of the likely broad scale signatures of the PDV, a Pan-Pacific domain is used in the primary analysis, which covers 120°E–60°W, 20°S–60°N. It should be noted that the choice of analysis domain, among others, might have led to the diversified PDV descriptions in literature. A Pan-Pacific analysis domain would, hopefully, facilitate the characterization of the PDV in the context of other modes of variability (e.g., ENSO) that have tropical origins. The point here is to use a single, consistent analysis technique to capture *all* the recurrent modes in the Pacific Ocean.

[1]United Kingdom Meteorological Office.

[2]Hadley Centre's sea ice and sea surface temperature data set.

[3]Scripps Institution of Oceanography.

[4]National Oceanographic Data Center.

[5]Six-month or three-month ocean heat content will probably be produced at NODC in 6–12 months (Levitus 2005, email communication).

[6]Intergovernmental Panel on Climate Change.

3.4 Rotated extended EOF

The EOF method has been widely used in geoscience to extract recurrent modes in the ocean and atmosphere. Mathematically, EOF decomposes the data field into a set of pairs called "modes", each pair consisting of a spatial pattern (also called EOF) that characterizes the mode in space and a time series (principal component or PC) that describes evolution of the spatial pattern. The first mode explains as much of the total variance as possible, the second mode explains as much of the remaining variance as possible, and so on. EOF is advantageous in that it allows an objective characterization of the modes both spatially and temporally, that it does not impose *a priori* periodicity. It is noted that pre-filtering is not uncommon in previous EOF-based studies; a robust EOF should, however, be such that it requires as few as possible prior manipulations of data to generate physically meaningful extractions. This is even more important in the context of possible ENSO-PDV superposition and may therefore not directly separable in the frequency space.

A variant of conventional EOF is the so-called extended EOF, which, instead of providing a single snap-shot of the spatial pattern, gives a sequence of such patterns at time interval Δt. The time interval is appropriately chosen such that the time sequence of the spatial patterns covers a significant portion of a variability episode. In the primary analysis, a five-member sequence at seasonal intervals is used.

By definition, the leading modes of EOF efficiently explain the variance of the *entire* domain being analyzed. This could however be a drawback when one or more physical modes dominate a part of the domain. Since the locally explained variance could be relatively low, the EOF may therefore fail to uncover the true physical patterns and/or their temporal variability. It can meanwhile lead to instability of the results as the analysis domain shrinks or expands. These deficiencies can be remedied by rotated EOF (REOF; Richman 1986), which yields more physically meaningful modes by relaxing the constraints of spatial and/or temporal orthogonality. Mathematically, rotated EOF is to find a linear combination of the leading modes retained from unrotated EOF for the sake of "simple structure". Physically, rotation is to redistribute the variables such that within each mode there are, ideally, a few large-valued variables which are clustered and all near-zero variables elsewhere. There are a variety of rotation techniques, among which a popular choice is VARIMAX. In VARIMAX-rotated EOF the spatial patterns will no longer necessarily be orthogonal, but the PC time series will remain orthogonal if suitably formulated. See Appendix A for a detailed mathematical treatment of the rotated extended EOF method used in this study.

3.5 Diagnostic modeling

A diagnostic model (Nigam and Chung 2000) will be used to dynamically assess the impacts of tropical and midlatitude anomalies at different stages of PDV evolution on local and remote near-surface circulation and fluxes. The model solves the steady primitive equations linearized about a zonally symmetric basic state. Eighteen full-σ levels are used, of which five are below 850 hPa. A semispectral horizontal representation is used, with 73 meridional grid points between the two poles, and 30 zonal waves (equivalent to a 6° Long × 2.5° Lat grid). The model has a reasonably realistic representation of vertical momentum and thermal

diffusion processes in the planetary boundary layer, which, given our interest at the ocean-atmosphere interface, will be of benefit. A more detailed model description can be found in Nigam and Chung (2000) and references therein. The model will be forced by observed SST and residually diagnosed 3-D diabatic heating, which will be carefully derived at different stages of PDV evolution.

3.6 Analysis tasks

3.6.1 PDV characterization

3.6.1.1 Primary analysis

The rotated extended EOF method (see Section 3.4 for a brief description and Section A for mathematical formulation) will be used to characterize spatiotemporal structures of PDV. The SST data set described in Section 3.3 will be investigated in the primary analysis; the analysis will be carefully designed with the expectation to extract all major low-frequency SST modes in the Pacific (e.g., ENSO, PDV, etc.) through one *single* step. Robustness of the rotated extended EOF method will be ascertained using sensitivity tests. The purpose of the primary analysis is to extract and describe PDV modal structures and evolution in context of other Pacific low-frequency variability, and meanwhile formulate a robust statistical method—i.e., rotated extended EOF—to be used in subsequent analysis of additional data sets and variables. With the primary analysis, expectation is to clarify and improve the somewhat ambiguous PDV descriptions (in terms of associated SST anomalies) in literature, as reviewed in Chapter 2.

3.6.1.2 Analysis of other data sets (observed and simulated)

The primary analysis will be repeated on a variety of observed SST data sets (e.g., COADS SST, NOAA extended reconstructed SST) to ascertain the stability/sensitivity of the diagnosed PDV structures. Longer periods (e.g., 1880-onward) will be analyzed for the same purpose.

Of equal interest is PDV representation in coupled climate models. Here, SST outputs of IPCC's 20^{th} century climate simulations will be analyzed. Priorities will, not surprisingly, be given to models having reasonably realistic representation of ENSO; other models will also be of interest, though.

3.6.1.3 Corroboration with other analysis techniques

The same data sets will be analyzed using (1) unrotated regular EOF, (2) rotated regular EOF and (3) canonical correlation analysis (or alternatively, singular value decomposition). Comparisons between rotated extended EOF (used in the primary analysis) and unrotated/regular EOF will help to identify advantages/disadvantages of each. Analysis of co-variability of SST and other oceanic/atmospheric variables will meanwhile be helpful to establish linkages between these variables.

3.6.2 PDV mechanisms

3.6.2.1 Lead/lag relationships

Lead/lag regressions and correlations are often revealing of interlinked processes. Though correlation does not necessarily reflect causality, it is helpful in the development and filtering of hypotheses on the mechanisms, which can then be further tested, e.g., via diagnostic modeling. Here key oceanic (e.g., SST, ocean heat content) and atmospheric (e.g., sea level pressure, surface wind, precipitation, etc.) variables will be analyzed for a more wholesome picture of PDV evolution. Comparisons will be made between observations and coupled simulations, not only for the interest of model validation; the more detailed information contained in model could on the other hand help to refine the results obtained from observations. Indeed, quite a few influential PDV theories are largely developed from modeling studies. The validity of these theories will be revisited, in observations and in different models.

3.6.2.2 Tropical-extratropical connections: role of atmosphere

Of interest is the impacts of SST anomalies at different stages of PDV on local and remote climate; particularly, decadal SST variations in the tropics and midlatitudes that are connected via atmospheric bridges. Diagnostic modeling is proposed to assess the implications of the PDV lead/lag relationships identified above. Not surprisingly, the focus will on the near-surface circulation response, and implications for surface fluxes and Ekman transports.

3.6.2.3 Tropical-extratropical connections: role of ocean

The PDV-covarying upper ocean heat content will be analyzed, in an effort to identify the oceanic linkages operative in PDV evolution. Volumetric heat balance will be evaluated, with relative importance of contributions from surface heat fluxes and subsurface processes of particular interest.

Chapter 4

Current Results

4.1 Primary Analysis

In this section, the leading modes identified in the primary analysis (described in Chapter 3) will be discussed. The number of modes rotated (here seven) is determined by a visual examination of the scree plot shown in Fig. 4.1; the stability of the analysis to the number of modes rotated will be further addressed in Section 4.2.

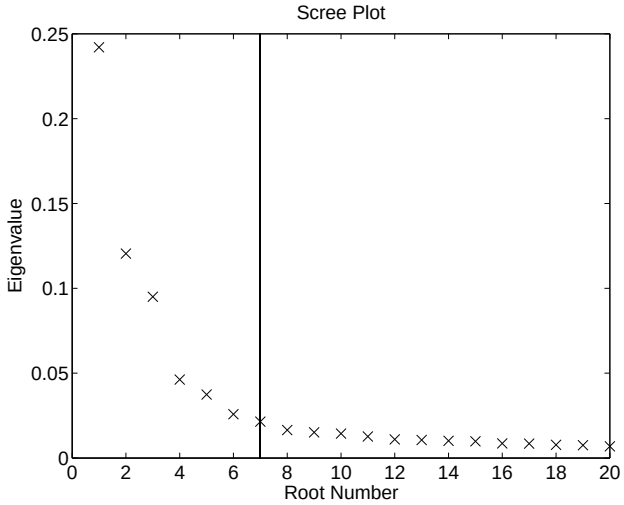

Fig. 4.1. Scree plot for the primary analysis. The eigenvalues are those before rotation.

A visual examination of the PC time series (shown in Fig. 4.2) immediately tells something interesting about the various modes they are associated with. Both PC1 and PC2, obviously lag-correlated, are characterized by significant interannual variations. It will be shown later that the two modes associated with PC1 and PC2 well capture the decaying and maturing phase of ENSO evolution, respectively. PC3 is characterized by a multidecadal to centennial trend, which is most outstanding after mid-1970's. Decadal and multidecadal variations are most significant in PC4 and PC6, respectively. Variations are however of smaller magnitudes and/or less prolonged in PC4 after 1970's. The well documented "regime shift" occurred

around 1976–77 is evident in PC6, but not in PC4. The names of the two PDV modes, i.e., Pan-Pacific and North Pacific, reflects the characteristic SST spatial patterns associated with them (to be discussed shortly). The physical nature of the fifth mode is not immediately clear by examining the PC time series, but will be shown to have captured the departure from "canonical" ENSO evolution (as depicted by, for example, the first two leading modes in this study). Finally, the seventh mode well captures the biennial variations, as is evident from the PC time series.

4.1.1 ENSO evolution

4.1.1.1 SST patterns

Unlike in regular EOF analysis which usually characterizes ENSO with a "snapshot" of its mature phase patterns (i.e., well-developed warmer-than-normal SSTs in equatorial central/eastern Pacific), the current analysis uncovers two modes associated with ENSO, each depicted by a time sequence, i.e., "evolution", of the associated SST patterns. Specifically, the second leading mode depicts the maturing of ENSO, while the first leading mode depicts the decaying of ENSO.

During the maturing phase of ENSO (Fig. 4.3; hereafter ENSO$^-$), positive SST anomalies are seen to first emerge in the equatorial eastern Pacific (off the coast of northern South America) as well as in the midlatitudes just off the U.S. west coast. Also seen is the development of negative SST anomalies in central North Pacific. These SST anomalies, positively- and negatively-signed, develop simultaneously over the seasons. Positive SST anomalies along the equator extend westward all the way to across the dateline, and meanwhile expand meridionally until finally merge with the same-signed SST anomalies off the U.S. west coast. Negative SST anomalies, on the other hand, display a standing-wave like behavior, developing in the central North Pacific about the center at $\sim$(180°, 30°N).

Unlike the maturing phase, the decaying phase of ENSO (Fig. 4.4; hereafter ENSO$^+$) is characterized by in-phase loss of amplitude in SST anomalies (both positively- and negatively-signed) basin-wide, except for the development of positive SST anomalies in western subtropical Pacific (and in tropical North Atlantic). Of interest is the rapid demise of positive SST anomalies in equatorial central/eastern Pacific in about one season.

Of special interest is the fifth leading mode, the most notable feature of which is an *eastward* development of positive SST anomalies along the equator (Fig. 4.5); this is opposite to a canonical ENSO evolution, and hence referred to here as the non-canonical ENSO mode (or ENSO Non-canonical). Accompanied by the eastward extension of positive SST anomalies is the shrinking of negative SST anomalies off the west coast of northern South America. In the corresponding principal component, greater amplitudes tend to be found in the post-regime-shift (1977-onward) period, an indication of nonstationarity. It is found that the principal component lags the NINO3.4 index in the pre-regime-shift period, whereas, more often than not, leads in the post-regime-shift period (not shown). It is imaginable that this mode strives to reverse the order of warming along equatorial Pacific from east-to-west to west-to-east after the regime shift. Using nonlinear EOF analysis based on neural network, Monahan (2001) found a non-canonical ENSO mode that is also characteristic of temporal nonstationarity relatable to the regime shift; the spatial evolution of that mode however

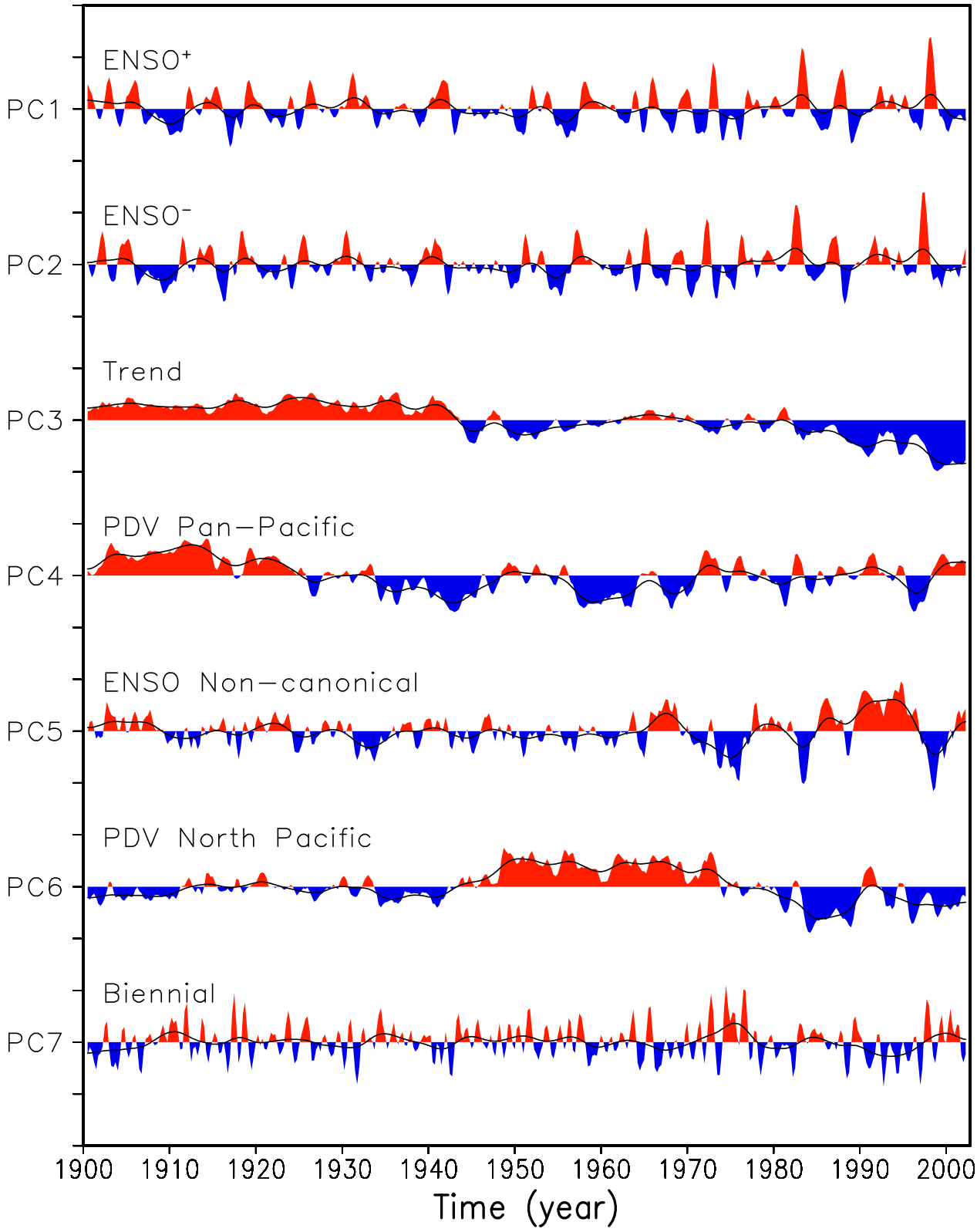

Fig. 4.2. The PC time series for the seven leading modes of Pacific SST variability during 1900–2002. Tick marks are drawn every three standard deviation on the vertical axis. Shadings are for original values. Curves are for heavily-smoothed versions of the same.

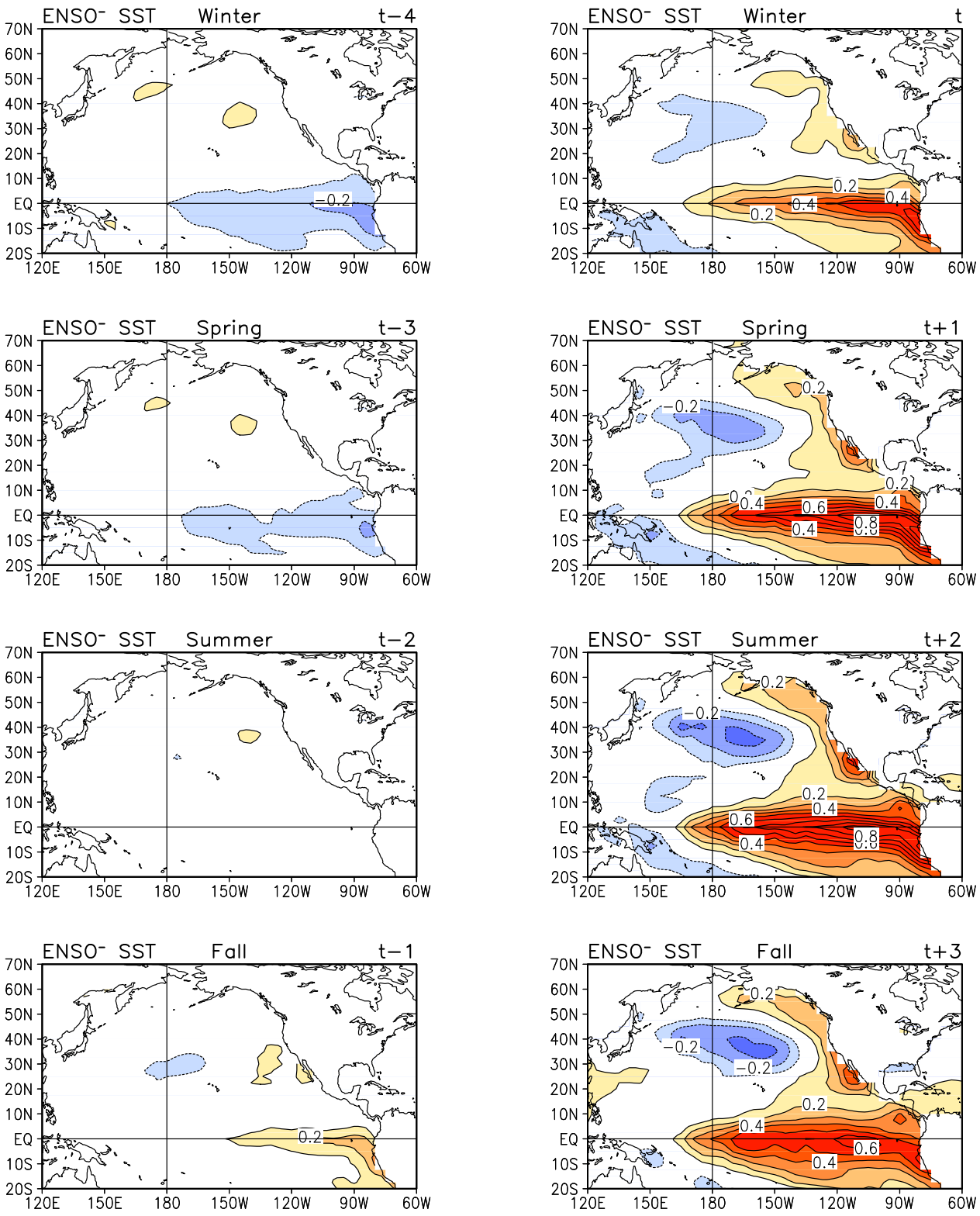

Fig. 4.3. The evolution of spatial patterns for the second leading mode (ENSO$^-$) of Pacific SST variability during 1900–2002. The analysis domain is 20°S–60°N, 120°E–60°W. The maps are obtained by regressing Pacific SSTs, suitably lagged, onto the associated PC time series. For example, "t-4" denotes the lag regression when SSTs lead the PC by 4 seasons, and so on. Positive values are solid, negative values are dashed, and zero values are omitted. Shadings are drawn along with contours for better visuability. Contour interval: 0.1°C.

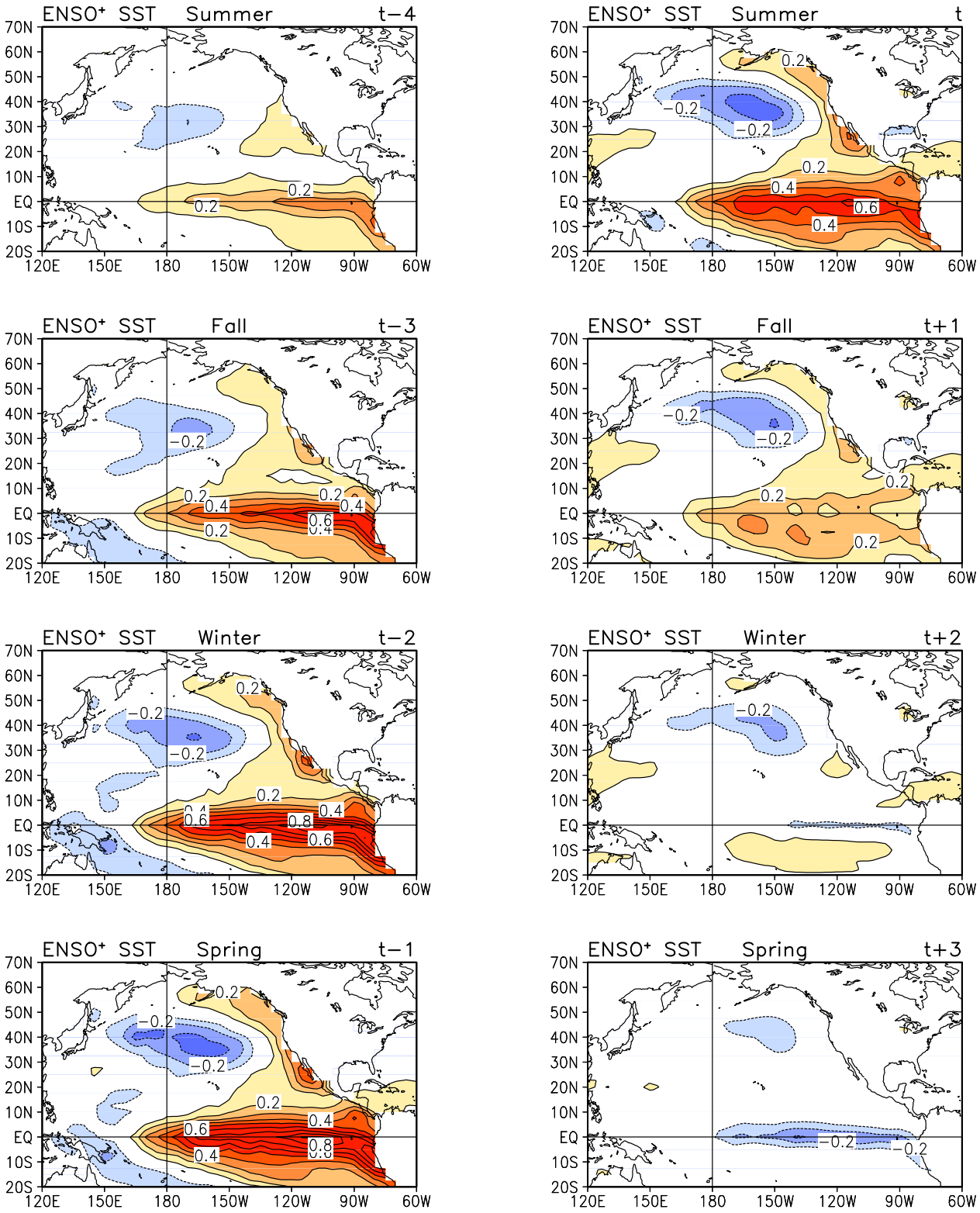

Fig. 4.4. Same as Fig. 4.3 but for the first leading mode (ENSO$^+$).

differs from the one described herein. How does this mode relate to PDV-caused ENSO modulation, if any, is worthy of further investigation.

4.1.1.2 ENSO time scale

The time scales for (canonical and non-canonical) ENSO variability already surface a little in Figures 4.3, 4.4 and 4.5, as described in Section 4.1.1.1. In this section, ENSO time scales are further investigated by looking at the autocorrelation structures of the NINO3.4 indices reconstructed from each of the ENSO modes and their combinations. The NINO3.4 indices are reconstructed as follows: first, seasonal SST anomalies (as a function of x, y and t) are reconstructed from multiplication of the simultaneous spatial pattern and associated PC time series. In case of modes combination, the two or three SST fields are then added. The NINO3.4 indices are then obtained by averaging the SST anomalies in the region of 170°W–120°W, 5°S–5°N. The same five NINO3.4 indices as reconstructed here will be used to analyze ENSO SST evolutions at the equator, and seasonal phase-locking, as well, in the following subsections.

Except for ENSO^{NC}, the reconstructed NINO3.4 indices all indicate a half-cycle of ∼2 years, as does the non-reconstructed one; the non-canonical ENSO mode, on the other hand, has a half-cycle of ∼3 years (Fig. 4.6). The reconstructed NINO3.4 indices for ENSO^{-} and ENSO^{+} are indeed characteristic of canonical ENSO evolution, i.e., an oscillation (so to speak) with a period of ∼4 years. The NINO3.4 index reconstructed from addition of ENSO^{-}, ENSO^{+} and ENSO^{NC} reproduce well the original version, especially after attaining the negative phase of ENSO; the effect of including the non-canonical ENSO mode in the reconstruction, after comparing with the reconstruction where the same mode is excluded, is to make the negative phase less connected to the positive phase, hence more reminiscent of the original NINO3.4 index. Indeed, the non-canonical ENSO mode does not attain significant negative values in the autocorrelation structure displayed, which, in addition to the longer time scale, suggests departures from canonical ENSO evolution.

4.1.1.3 Seasonal phase-locking

One characteristic of ENSO evolution is its synchronization to the seasonal cycle (referred to as "seasonal phase-locking"). More precisely, the mature phase of ENSO (characterized by well-developed SST anomalies in equatorial central/eastern Pacific) tends to occur during boreal winters. Here seasonal phase-locking is assessed for the same five reconstructed NINO3.4 indices as defined above. The purpose is to ascertain proper seasonality in the reconstructed SSTs. The non-reconstructed NINO3.4 index is, again, used as a target for the assessment.

Not surprisingly, the non-reconstructed NINO3.4 index has largest variability in winter. Less largest variability is observed in fall. Considerably smaller variability is observed in both spring and summer. Noteworthy is the rapid growing (decaying) during summer-to-fall (winter-to-spring). The ENSO^{-} mode, much as expected, has largest variability in winter and in spring, characterized by the winter-to-spring growing and summer-to-fall decaying (i.e., leading NINO3.4 by two seasons). The ENSO^{+} mode appears to be leading ENSO^{-} by one season, which turns out to be an artifact of having only one year on the time axis;

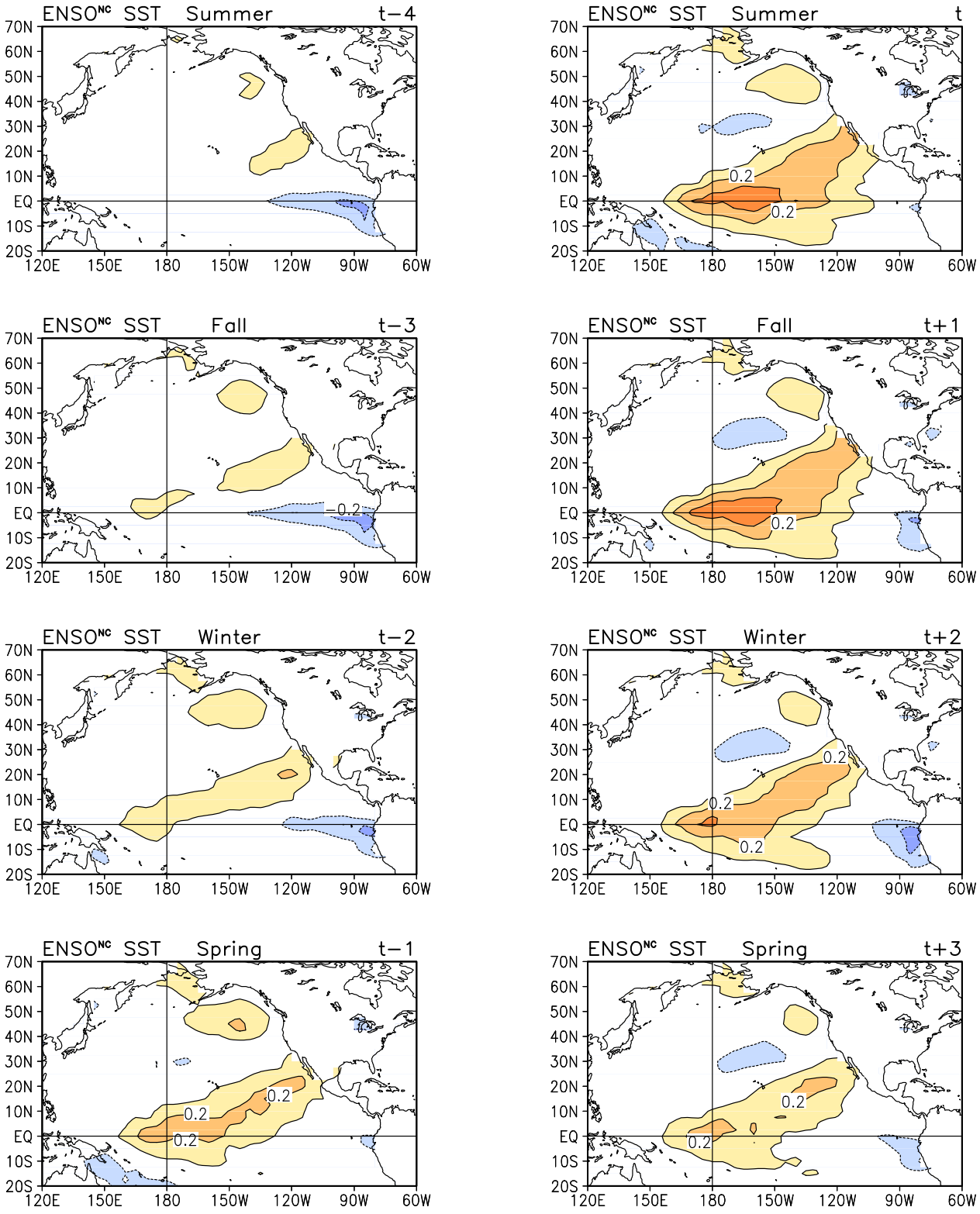

Fig. 4.5. Same as Fig. 4.3 but for the fifth leading mode (ENSO Non-canonical).

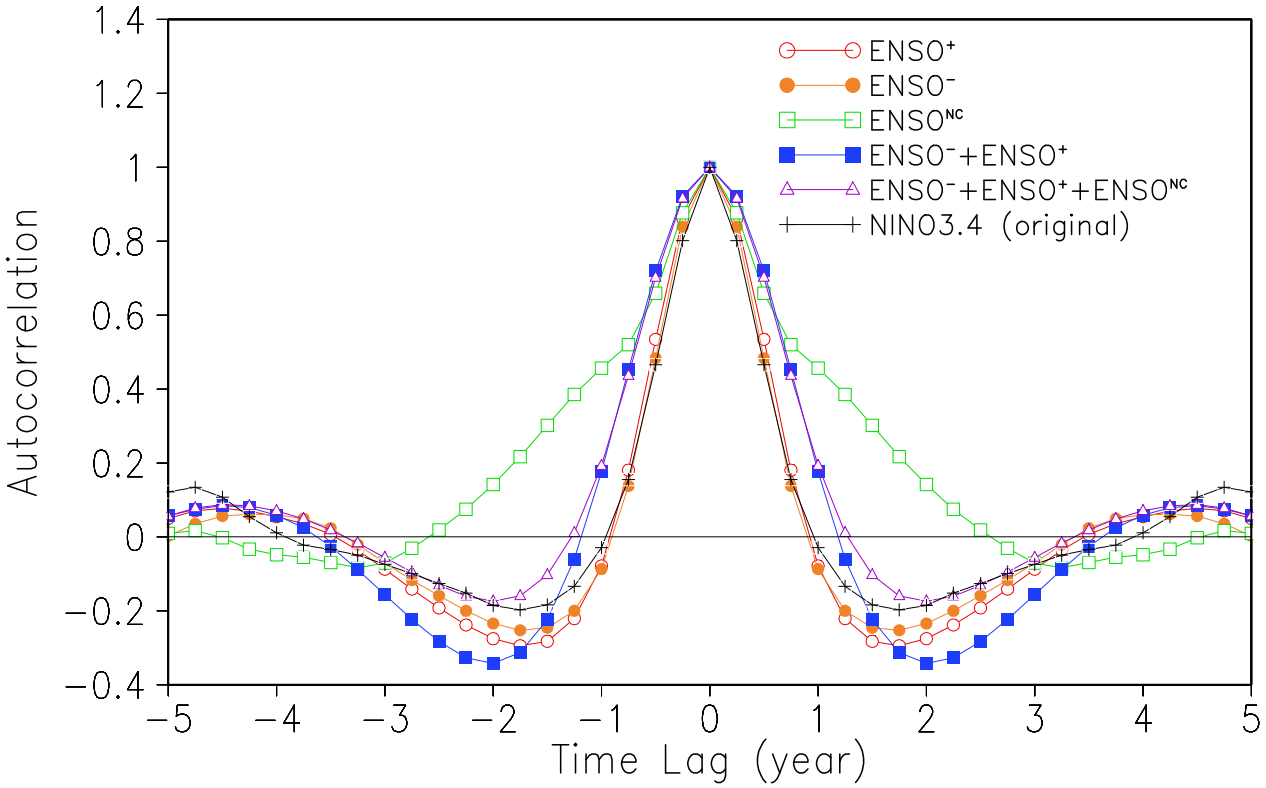

Fig. 4.6. Autocorrelation of reconstructed NINO3.4 indices for the ENSO$^-$, ENSO$^+$, ENSO^{NC} mode and their combinations; labels indicate the mode(s) involved in the reconstruction. Refer to the text for reconstruction procedures. The NINO3.4 index calculated from non-reconstructed (i.e., original) SST anomalies is also shown (plus signs), for reference.

it actually lags ENSO$^-$ by three seasons, which can be easily ascertained by lag correlation of the two time series. The non-canonical ENSO mode has similar seasonality to the non-constructed NINO3.4 index, except with reduced amplitudes. Not surprisingly, seasonality is greatly suppressed in the SSTs reconstructed from addition of ENSO$^-$ and ENSO$^+$ (since the two modes are lag-correlated, peaking in different seasons); seasonality is recovered to reasonable extent when ENSO^{NC} is included in the reconstruction. Full amplitudes in seasonality however cannot be reproduced by any of the reconstructions due to the omission of higher-frequency variability (the biennial mode, for example).

4.1.1.4 SST evolution at the equator

SST evolution at the equator can be shown to have different patterns across the 1976 regime shift: during 1900–1976, it is characterized by a east-to-west growth (and decay, as well) of amplitudes (Fig. 4.8d); the direction is reversed during 1977–2002, when SST anomalies first emerge from near the dateline, and reach the eastern Pacific in ∼1 season (Fig. 4.8g). The century-long pattern (1900–2002), not surprisingly, is a reconciliation of the two: SST anomalies still grow from the eastern Pacific, but the westward propagation is much less significant than during 1900–1976 (Fig. 4.8a).

It is then of interest to see whether and to what extent this change in SST can be

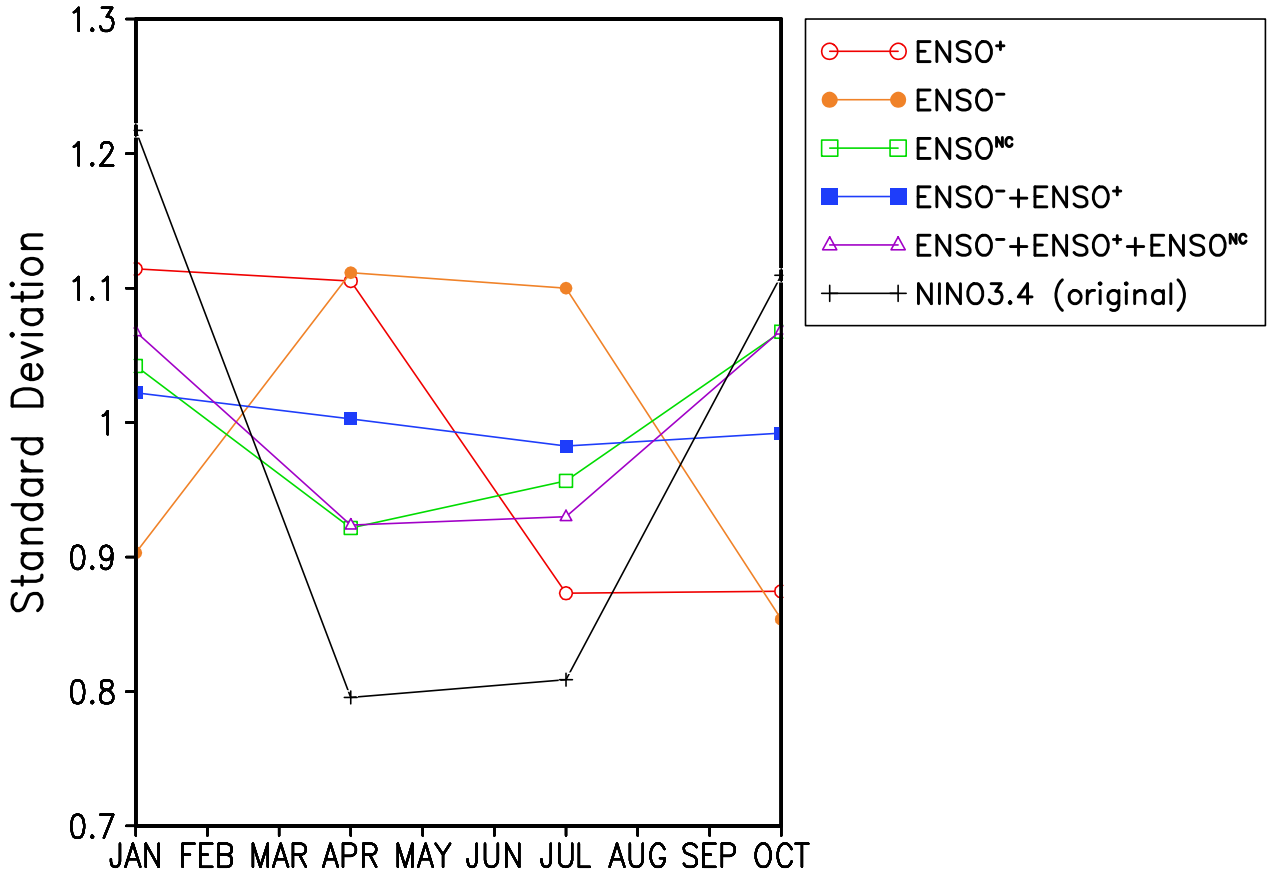

Fig. 4.7. Seasonal phase-locking of ENSO variability. Standard deviations of reconstructed and non-reconstructed NINO3.4 indices (same as in Fig. 4.6; see text for details in reconstruction) are shown for each of the four seasons.

reproduced by SST anomalies reconstructed from the ENSO modes identified in the current analysis. SST evolution is quite similar across the regime shift when only ENSO$^-$ and ENSO$^+$ are included in the reconstruction: westward growth of amplitudes are observed during both the pre- and post-regime-shift periods (and during the whole length, as a result; see Fig. 4.8b,e,h), except that larger amplitudes are observed during the latter period. Only when ENSO^{NC} is included in the reconstruction can the change in SST evolution be reproduced, to reasonable extent (see Fig. 4.8f,i). The century-long pattern are also better reproduced in this case: maximum amplitudes are more away from the west coast (Fig. 4.8c), as is in the non-reconstructed case, the target (Fig. 4.8a).

4.1.2 PDV: Pan-Pacific and North Pacific

The fourth and sixth modes, both PDV-related, have quite different SST spatial patterns. The mature phase of the fourth mode (Fig. 4.9; hereafter PDV Pan-Pacific) is characterized by a limited area of positive SST anomalies in the central North Pacific (centered east of the dateline), surrounded by negative SST anomalies of much greater magnitudes along the U.S. west coast; the negative SST anomalies extends all the way to the tropical western North

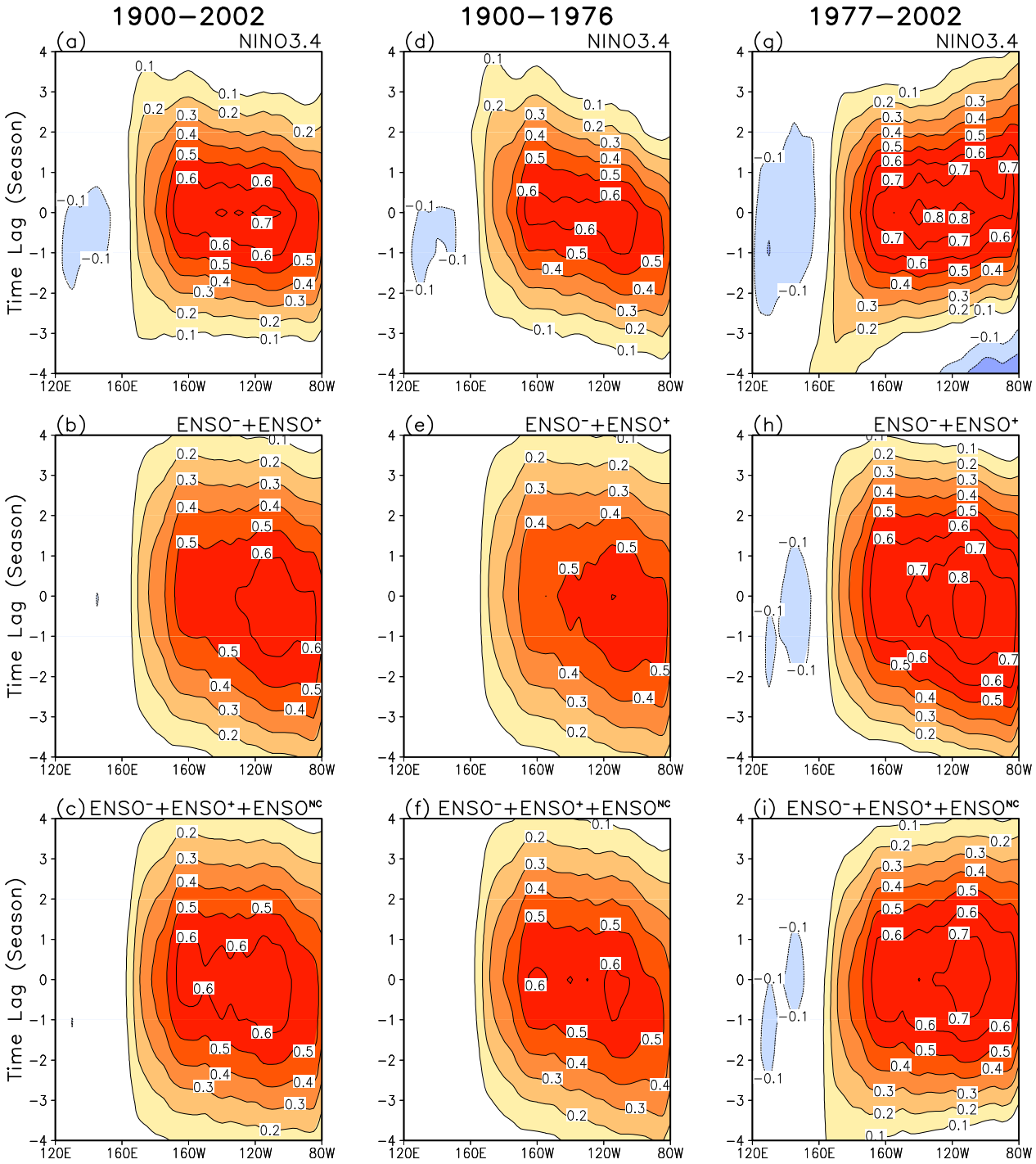

Fig. 4.8. ENSO SST evolution at the equator. Lead/lag regressions of SSTs, averaged between 5°S–5°N, are shown over a period of 9 seasons. The maps are obtained by regressing the SST anomalies, either original (first row) or reconstructed (second and third rows; refer to labels on top of each panel for the modes involved in the reconstruction), onto the NINO3.4 index calculated from the same version of SSTs. Three time periods are being examined, i.e., 1900–2002 (left column), 1900–1976 (central column), and 1977–2002 (right column). Positive values are solid, negative values are dashed, and zero values are omitted. Shadings are drawn along with contours for better visuability. Contour interval: 0.1°C.

Pacific. Also seen are some weak SST anomalies, negatively signed, in tropical North Atlantic. Noteworthy is the lack of equatorial SST signature in central/eastern Pacific, especially in the context of possible ENSO-PDV superposition as suggested by some previous studies. The overall evolution features a development of negative SST anomalies stronger than $-0.3°$C along the U.S. west coast in about 4 years, which then decays in an opposite manner. The development and decay of positive SST anomalies in central North Pacific, on the other hand, is more sudden; the whole process takes place in less than a year. Note the cooling along and off the U.S. west coast leads the warming in central North Pacific.

The mature phase of the sixth mode (Fig. 4.10; hereafter PDV North Pacific), on the other hand, is characterized by a zonally elongated band of positive SST anomalies (much stronger and of greater extent than those associated with PDV Pan-Pacific) in North Pacific with maximum at either side of the dateline. Tropical signatures does exist, with considerable magnitude and extent especially before the positive SST anomalies in North Pacific reach the peak. Further, the development and decay of negative SST anomalies in the equatorial eastern Pacific seem to lead their counterpart in North Pacific by about 1 year. It is not immediately clear whether the SST anomalies here in the equatorial eastern Pacific is related to ENSO.

To check the physicality of the two PDV modes, correlations are calculated between the associated principal components and the 100 physical/biological time series assembled by Hare and Mantua (2000) in the North Pacific Ocean and Bering Sea during 1965–1997. It turns out that the North Pacific mode is more evidenced biologically (see Table 4.1 for selected results) within the 100 time series, whereas the Pan-Pacific mode is more evidenced physically (not shown) within the same data set. The general high correlations found preclude the possibility that one or both of the PDV modes are merely statistical artifacts.

Table 4.1. Correlations between the principal components of the two PDV modes and selected biological time series during 1965–1997. All time series are annually resolved.

	PP		NP
Eastern Pacific zooplankton biomass	−0.54	Gulf of Alaska halibut recruitment	−0.74
British Columbia coho salmon catch	0.42	West Coast mackerel recruitment	−0.73
E. Bering Sea flathead sole recruitment	−0.39	Central Alaska chinook catch	−0.68

Note: PP=Pan-Pacific mode, NP=North Pacific mode.

4.1.3 Biennial variability

As seen, the PC time series associated with the seventh mode well captures biennial SST variability. The evolution of this mode (Fig. 4.11; hereafter the biennial mode) involves a succession of positive/negative SST anomalies emerging from equatorial eastern Pacific and over the time extending towards/across the dateline. Also evident is the demise of positive SST anomalies in the central north Pacific as same-signed SST anomalies build up in the equatorial eastern Pacific. Except for the 2-yr cycle, the SST evolution of this mode is not without some similarity to that of ENSO (cf. Figs. 4.3,4.4), indicative of possible linkages between the two. Biennial mode with similar spatiotemporal structures has also been found in previous studies (e.g., Barnett 1991).

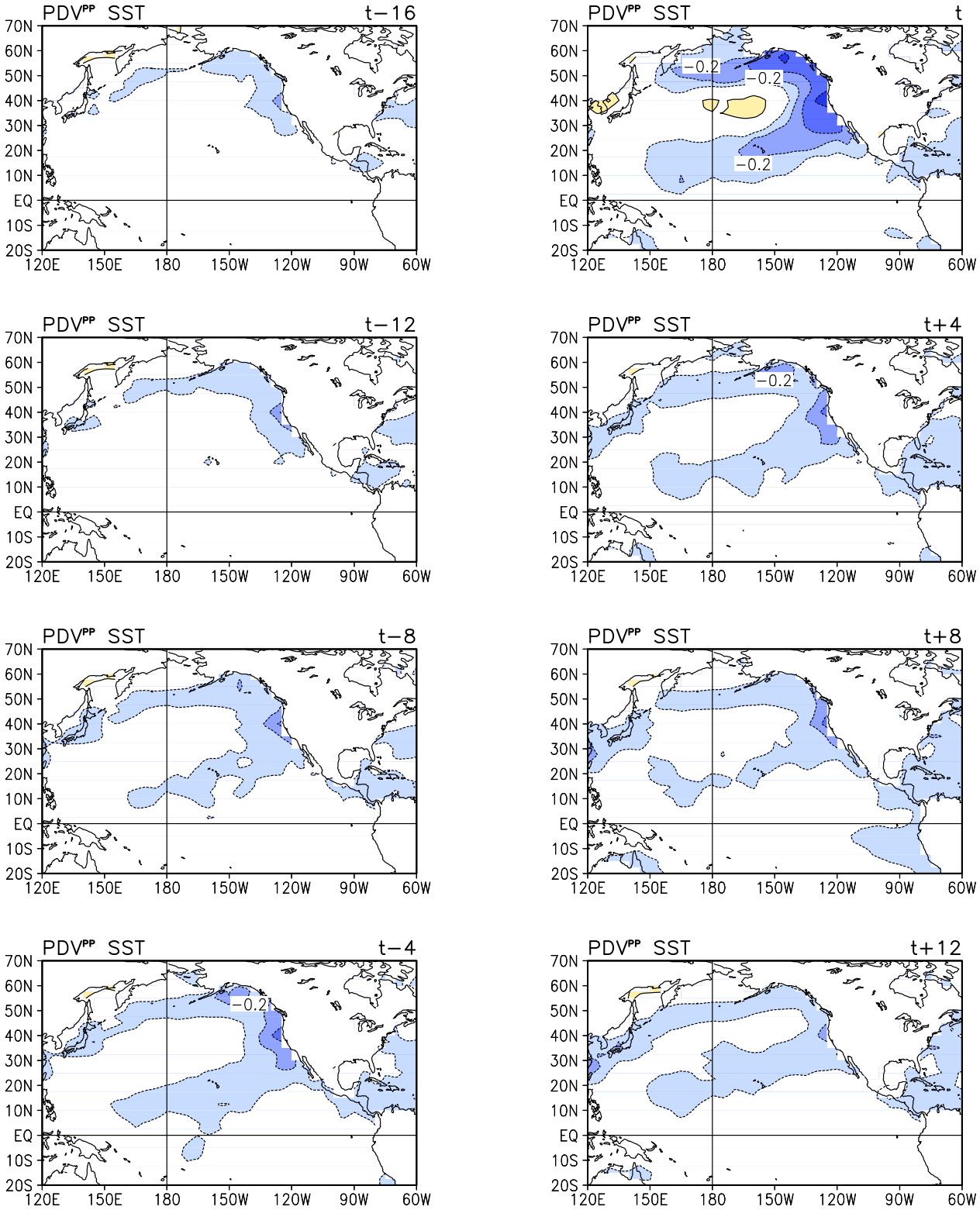

Fig. 4.9. Same as Fig. 4.4 but for the fourth leading mode (PDV Pan-Pacific). Note lag regressions are now shown at 4-season intervals.

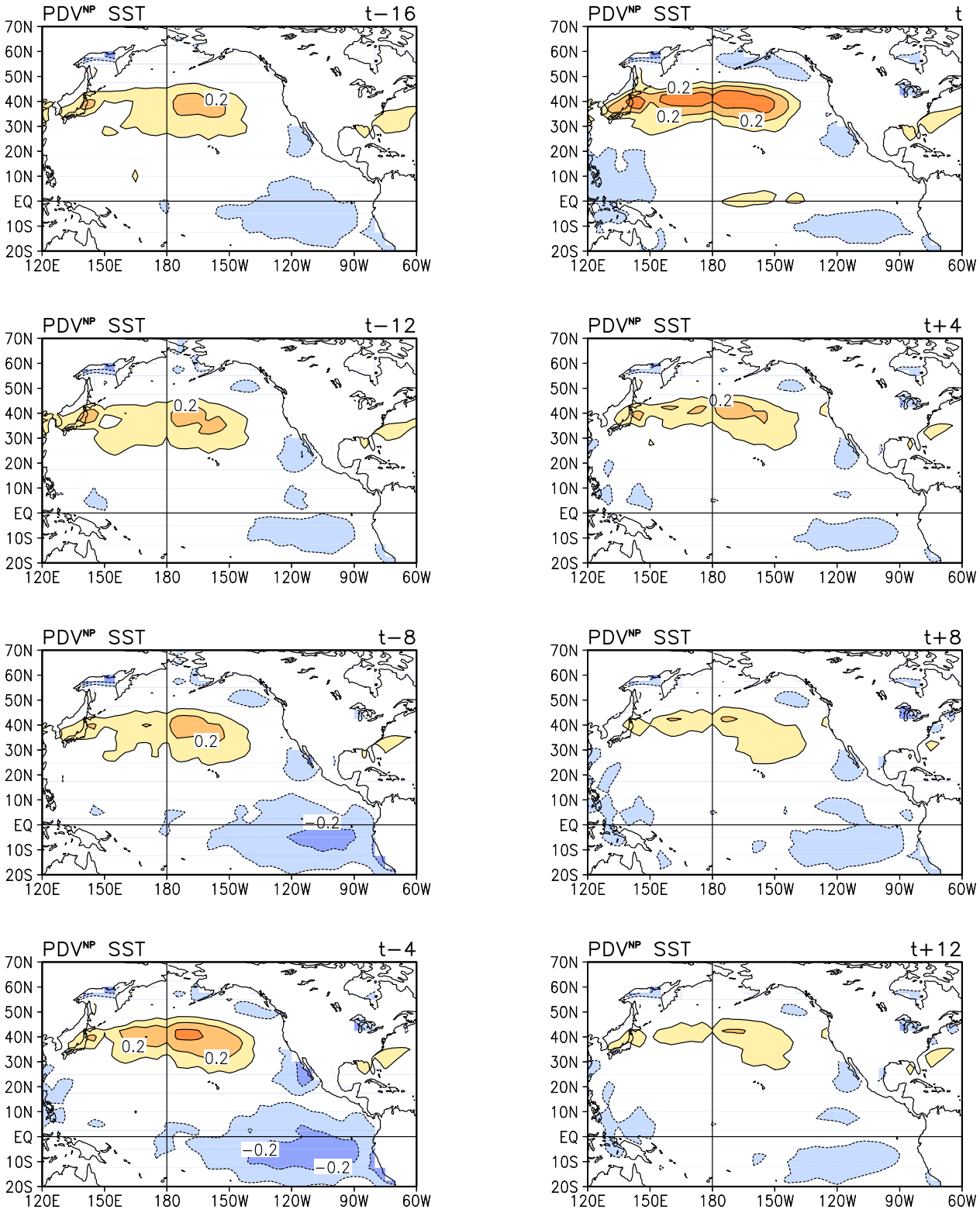

Fig. 4.10. Same as Fig. 4.9 but for the sixth leading mode (PDV North Pacific).

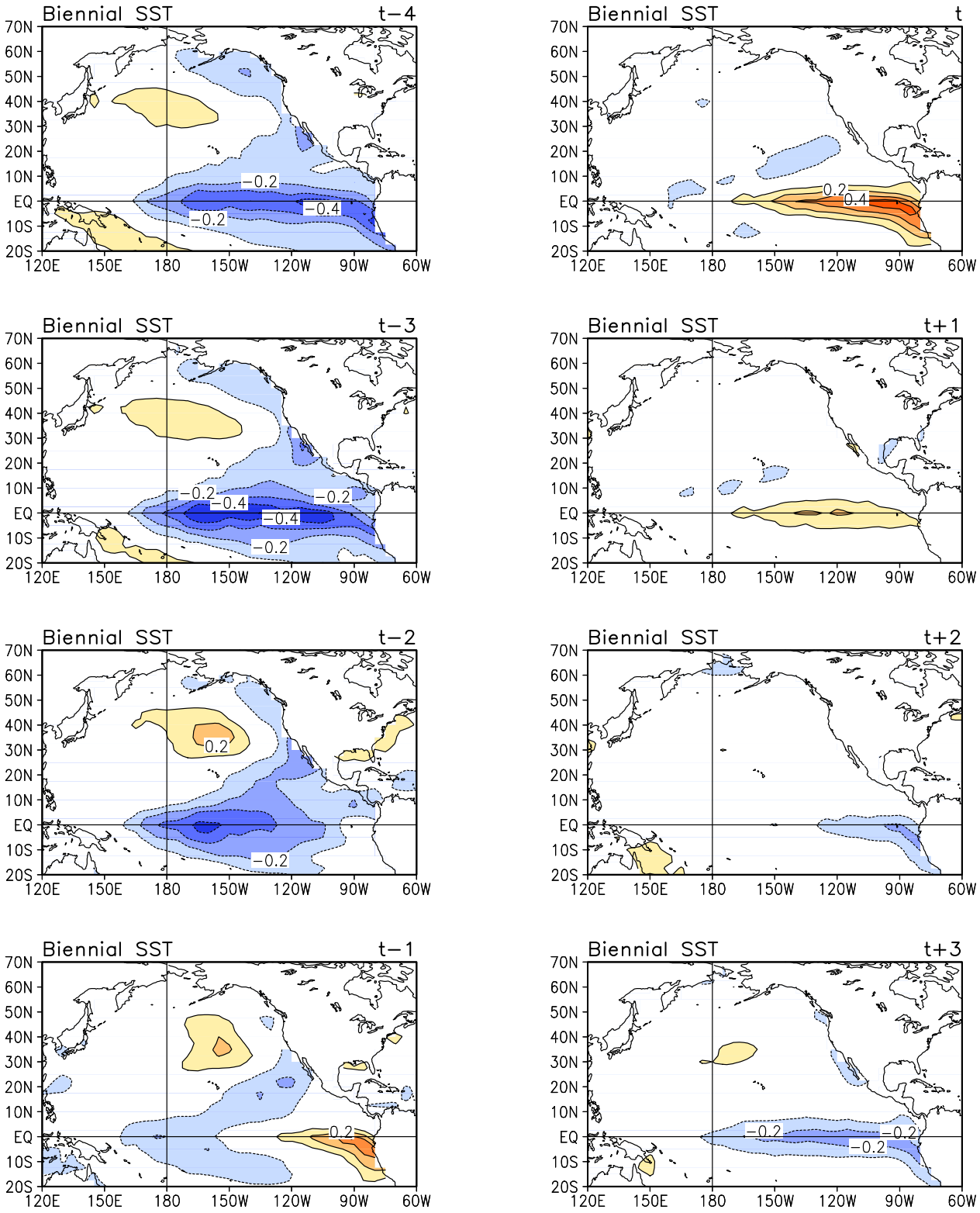

Fig. 4.11. Same as Fig. 4.3 but for the seventh leading mode (the biennial mode).

4.1.4 Trend

The third mode (not shown; hereafter the trend mode) is characterized by a broad band of negative SST anomalies across the northern North Pacific basin as well as the equatorial western Pacific, which has no obvious time evolution. Also present is one or two patches of positive SST anomalies in the equatorial central Pacific. Of interest is the associated PC time series in context of PDV: the time series can be generally partitioned into three regimes, i.e., pre-1940's, 1940's–1970's, and post-1970's, during which the PC is broadly positive, neutral, and negative, respectively.

4.1.5 Inter-relationship between low frequency variability

The simultaneous correlations between the principal components associated with the above modes are all zeros, by definition. The modes could however be correlated at certain lead/lags.

Shown in Fig. 4.12 is the lead/lag correlations between the ENSO^{+} mode/PDV^{NP} mode and all seven modes identified from the primary analysis. Significance is inferred whenever correlation coefficients exceed ± 0.6. Obviously, the ENSO^{-} mode leads the ENSO^{+} mode by about 3 seasons, and is the only mode significantly correlated to the latter on interannual time scales. The biennial mode does show some correlation to the ENSO^{+} mode, though, at a lag of about 0.5 year. The auto-correlation structure of ENSO^{+} meanwhile well conforms to the approximate mean period of ENSO (i.e., 4 years). On decadal time scales, the most significantly interlinked modes are the Pan-Pacific mode and North Pacific mode; the former leads the latter by about 44 years with correlation coefficient of 0.69. The trend mode also shows some correlation to the North Pacific mode at a lead/lag of about 30–40 years, but with less significance. Note that SST variability associated with ENSO is not *directly* linked to that associated with PDV, or vice versa.

4.1.6 Comparisons with other analyses

The ENSO and PDV modes have been discussed in many previous studies using regular EOF analysis, either unrotated or rotated. The results are however not always directly comparable due to different selection of data set, analysis domain/period, and computational procedures as well. Two additional analysis, namely, unrotated regular EOF and rotated regular EOF, are therefore conducted, with everything kept the same as in the primary analysis except for the EOF formulation.

Shown in Fig. 4.13 are the principal components associated with ENSO from all three types of EOF analysis, superposed on the NINO3.4 index—a well-defined ENSO index. In the two regular EOF analysis, ENSO is both captured by the first leading mode; in the rotated extended EOF analysis, it is captured by the first *and* second leading modes, as already discussed previously. In all cases, the principal components correlate well with the NINO3.4 index, except that in rotated extended EOF, PC1 leads the latter by 1 season, while PC2 lags by 2 seasons. Specifically, the anomalously strong El Niño during 1982–83 and 1997–98 are nicely captured by all. Taking the results here as well as those in previous studies, it may well be concluded that the ENSO mode, due to its well established ocean-atmosphere dynamics and strong signal, is a rather stable mode that is barely sensitively to

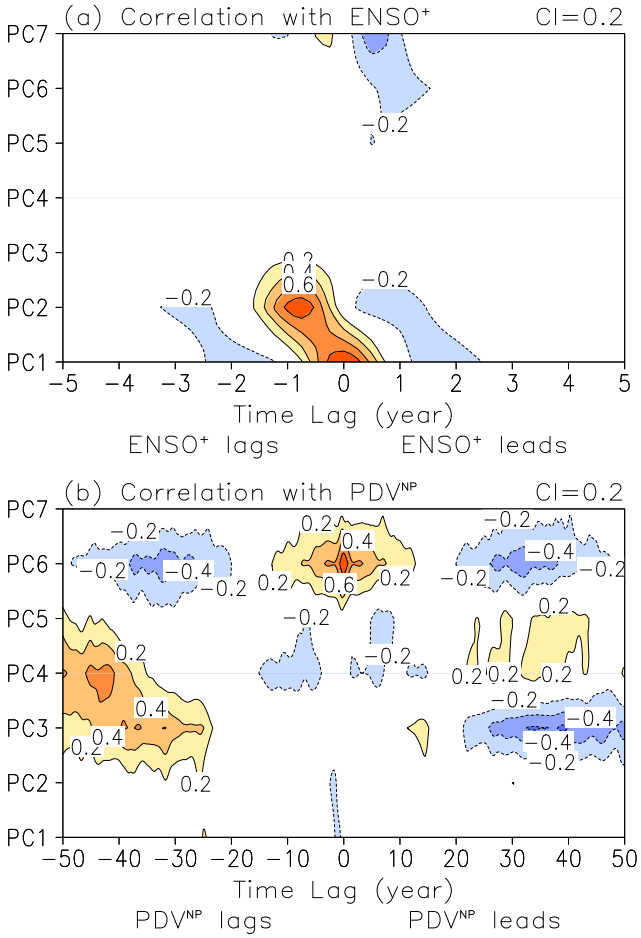

Fig. 4.12. (a) Lead/lag correlations between the ENSO$^+$ mode and all seven modes identified from the primary analysis. (b) Same as (a) but for the North Pacific mode. Note the time axes in (a) and (b) are on difference scales.

analysis techniques.

Much different is the case of PDV, which already involves considerable ambiguity in literature. That PDV may involve more than one mode, as does in our analysis, further complicates the problem. Shown in Fig. 4.14 are the principal components associated with the Pan-Pacific mode from the three types of EOF analysis, superposed on the PDO index (Mantua et al. 1997)—now a well accepted index of North Pacific variability. All time series are heavily smoothed to suppress any interannual variations. A similar plot for the North Pacific mode is shown in Fig. 4.15, for comparison.

The Pan-Pacific mode is present in all three analyses, but with rather different characteristics (Fig. 4.14). The principal component and associated spatial pattern (not shown) are most akin to those of Mantua et al. (1997)'s PDO when unrotated regular EOF is used, much as expected since the same technique is used in Mantua et al. (1997). In rotated extended EOF, the principal component is essentially uncorrelated with the PDO index. The associated spatial pattern (see Fig. 4.9) also deviates much from Mantua et al. (1997)'s PDO (their Fig. 2a) but however reminiscent of Barlow et al. (2001)'s PDO (their Fig. 2b). The

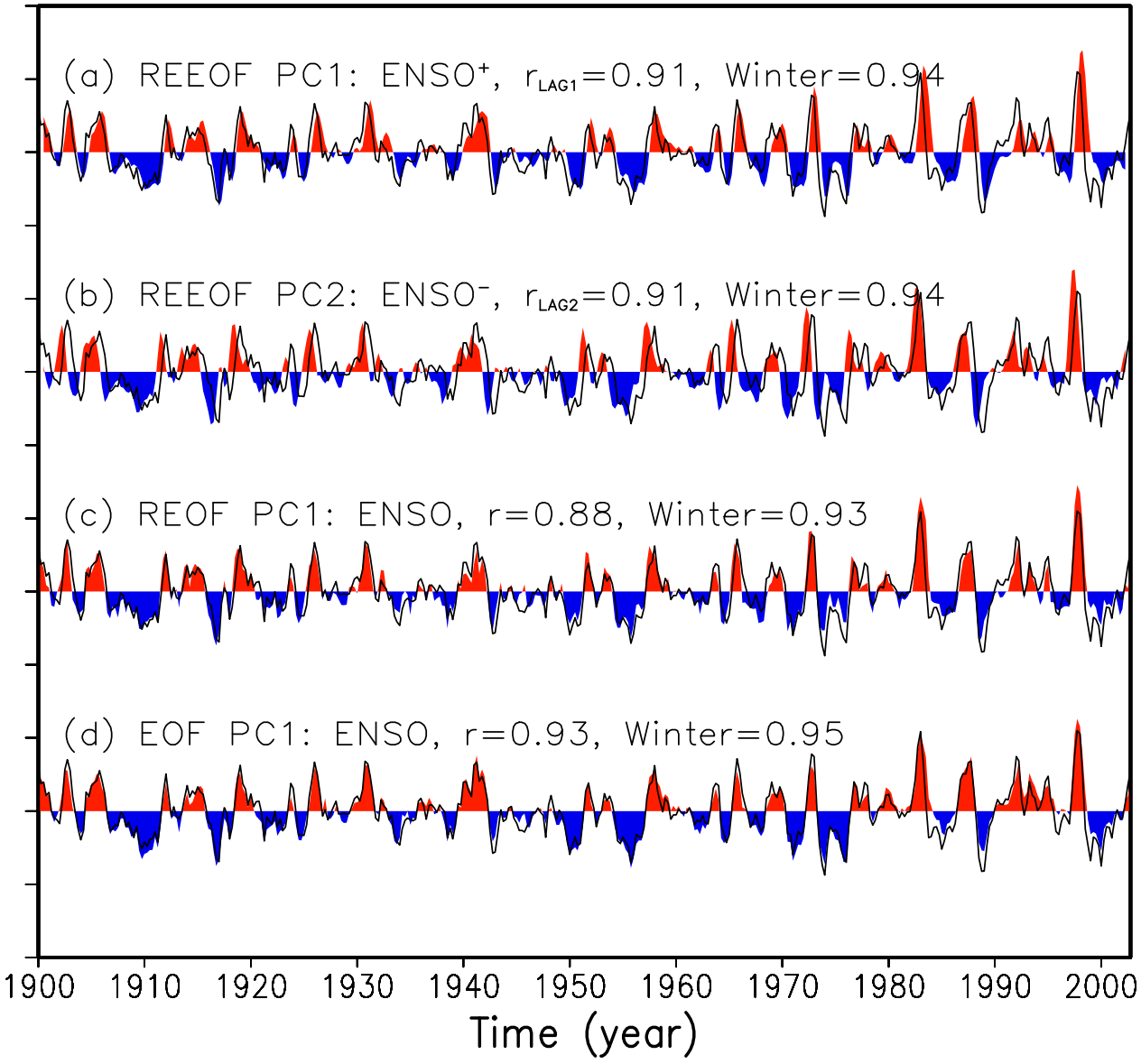

Fig. 4.13. The principal component (shading) associated with ENSO from (a),(b) rotated extended EOF, (c) rotated regular EOF and (d) unrotated regular EOF. Superposed is the normalized NINO3.4 index (curves). Indicated above each curve is the all-season correlation as well as winter correlation between the principal component and the NINO3.4 index. Note correlations shown in (a) is lag-correlations when PC1 leads NINO3.4 by 1 season, while those shown in (b) is lag-correlations when PC2 lags NINO3.4 by 2 seasons. Tick marks are drawn every three standard deviation on the vertical axis.

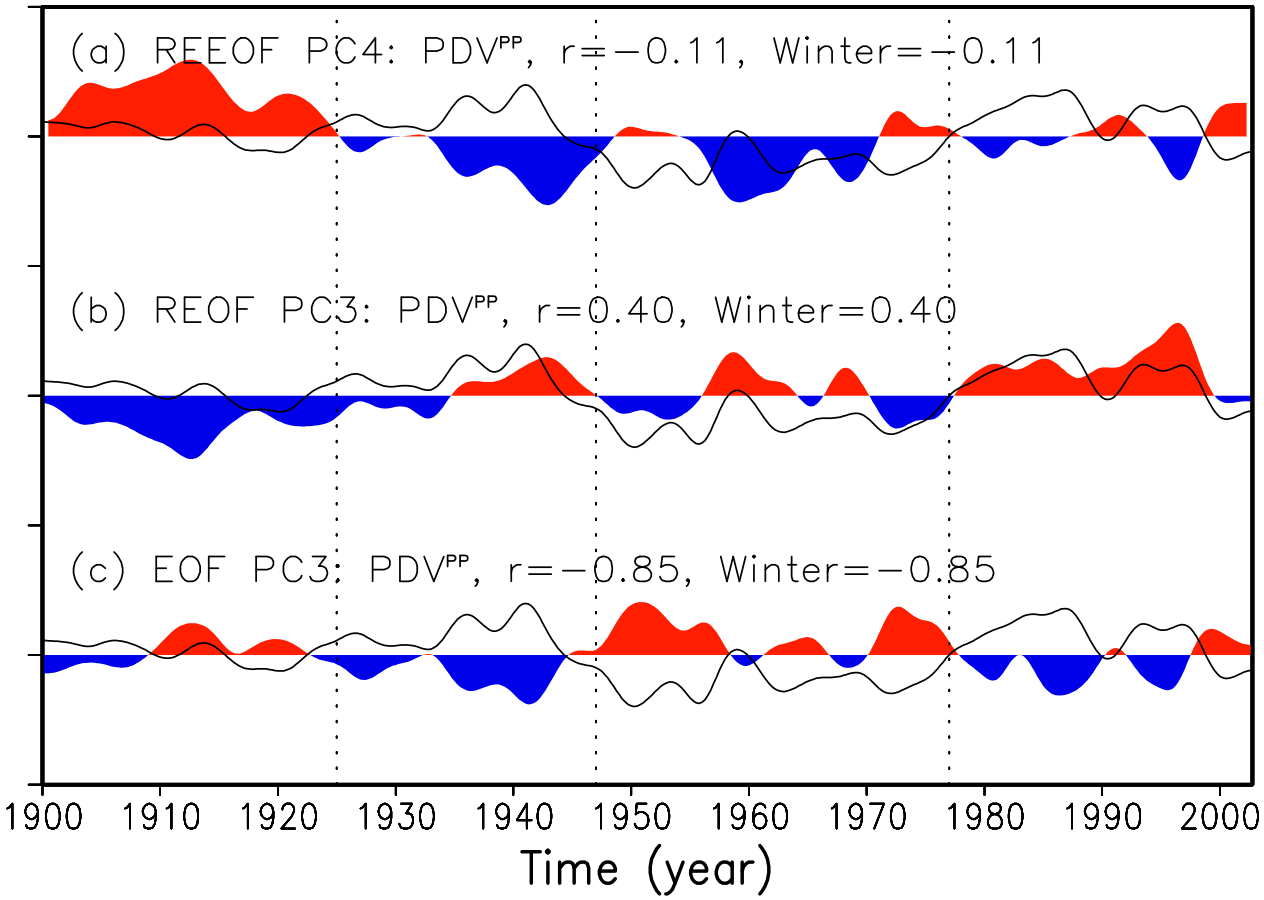

Fig. 4.14. The principal component (shading) associated with the Pan-Pacific mode from (a) rotated extended EOF, (b) rotated regular EOF and (c) unrotated regular EOF. Superposed is the PDO index (curves). All time series are heavily smoothed. Indicated above each curve is the all-season correlation as well as winter correlation between the principal component and the PDO index. Dotted lines indicate the regime shifts proposed by Mantua et al. (1997). Tick marks are drawn every three standard deviation on the vertical axis.

result from rotated regular EOF lies somewhere between the above two analyses. Note that the proposed regime shift around 1925 (Mantua et al. 1997; Minobe 1997) does seem to appear in rotated extended EOF, with even greater significance than in the PDO index; the other two proposed regime shifts are however absent from the former.

Unlike the Pan-Pacific mode, the North Pacific only exists in the rotated cases (Fig. 4.15). The principal component from rotated extended EOF correlates well with the PDO index, if heavily smoothed. The associated spatial pattern is meanwhile reminiscent of Mantua et al. (1997)'s PDO and Barlow et al. (2001)'s North Pacific mode. Moreover, the proposed regime shifts around 1947 and 1977 are both evident in the principal component; less evident is the one around 1925, though. Comparison of Fig. 4.15a,b shows that rotation alone does not seem to be sufficient to characterize the North Pacific mode temporally. Taking together, both the Pan-Pacific mode and the North Pacific mode identified in our primary analysis have their significance with respect to regime shifts; not surprisingly, only the North Pacific mode here is correlated to Mantua et al. (1997)'s PDO since they both have weight in the North Pacific. The point here is that with rotated extended EOF we are able to identify two

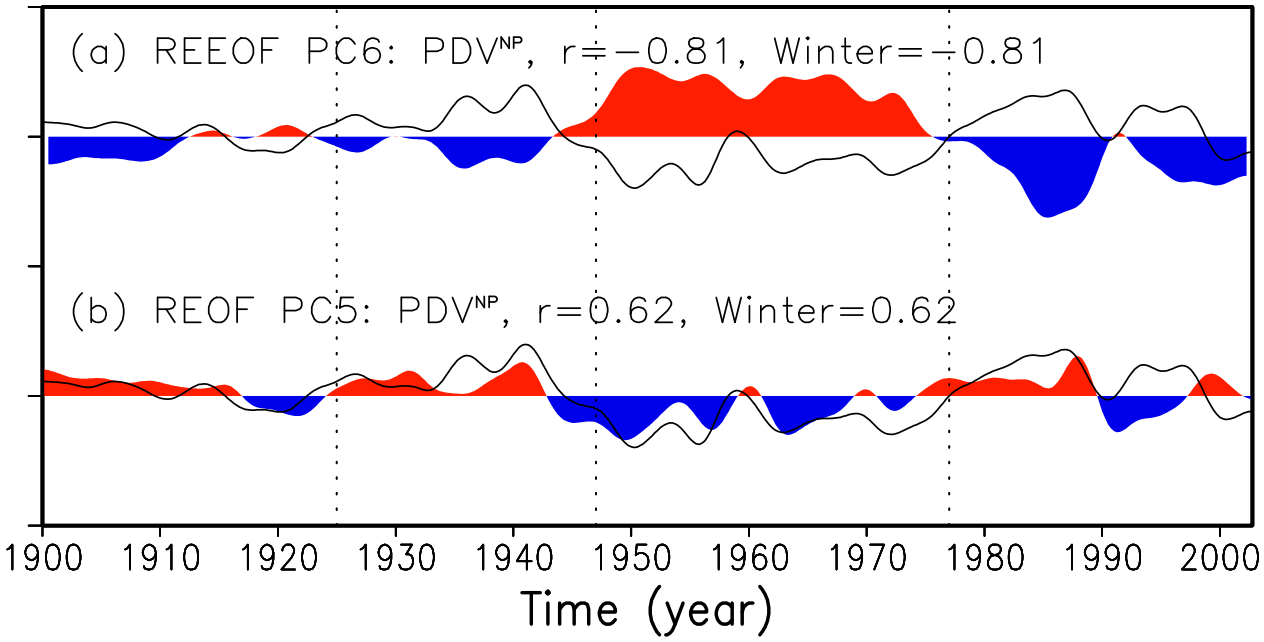

Fig. 4.15. The principal component (shading) associated with the North Pacific mode from (a) rotated extended EOF and (b) rotated regular EOF. Superposed is the PDO index (curves). All time series are heavily smoothed. Indicated above each curve is the all-season correlation as well as winter correlation between the principal component and the PDO index. Dotted lines indicate the regime shifts proposed by Mantua et al. (1997). Tick marks are drawn every three standard deviation on the vertical axis.

PDV modes with different geographical emphasis and evolution characteristics, each of which has considerable observational evidences.

4.2 Sensitivity tests

The primary analysis described in the previous section is perturbed in several ways to ascertain the stability of the modes identified therein. Listed in Table 4.2 is the name and design of these sensitivity tests alongside the primary analysis. Each sensitivity test[1] is intended to address a specific aspect of the primary analysis, including the analysis domain (A359), analysis period (A350), period used in the definition of climatology (A357), number of eigenvectors rotated (A353), and lag size (A361). The analysis domain should normally be carefully chosen in unrotated EOF such that it reflects the physical domain the mode in interest is operative since unrotated EOF, by definition, efficiently explain the variance in the *entire* analysis domain. This constraint on the analysis domain is expected to relaxed in case of rotated EOF, such as the primary analysis in this study. In case a long time period is analyzed, the definition of climatology could also be an issue; climatology may not be well defined during the early years when observations are not of equal quality. Probably the most important parameter in rotated EOF is the number of modes included in the rotation, which should be sufficiently large such that the analysis will not be unduly sensitive to small

[1]Any individual test actually represents a group of tests in which the same parameters are altered to slightly different extent.

perturbations in this parameter. It however should not be too large for great signal-to-noise ratio as well as efficient computation. Except in A361, the procedures for calculation is all the same as in the primary analysis. A361 is a special analysis in which the SST field is first partially reconstructed from the EOFs and PCs in A351 (the primary analysis) with the biennial mode and the ENSO modes (both canonical and non-canonical) dropped out, and then subject to a rotated extended EOF analysis with 6-month lags and 3 modes rotated (since only 3 modes are retained in the reconstruction). The purpose of this analysis is to address the concern that the 1-yr time span (5 lags at 3-month intervals) in the primary analysis could be too short to robustly extract variability patterns at decadal time scales.

Table 4.2. Name and design of the sensitivity tests. A351 is the primary analysis. The "Pacific" domain is defined as 120°E–60°W, 20°S–60°N. The "Indo-Pacific" domain is defined as 30°E–60°W, 20°S–60°N.

Name	Domain	Period	Climatology	Rotated	Lag Size
A351	Pacific	1900–2002	1900–2002	7	3 mo
A359	Indo-Pacific	1900–2002	1900–2002	7	3 mo
A350	Pacific	1945–2002	1945–2002	7	3 mo
A357	Pacific	1900–2002	1945–2002	7	3 mo
A353	Pacific	1900–2002	1900–2002	9	3 mo
A361	Pacific	1900–2002	1900–2002	3	6 mo

The sensitivity tests (except A361) all reproduced the leading seven modes identified in the primary analysis, except some are in different orders (Table 4.3). The high correlation (all near 1 with only a few exceptions) in Table 4.3 attest to the stability of the primary analysis in all tested aspects. Not surprisingly, the ENSO$^+$ mode explains the most variance in all cases. Except in A353, the biennial mode explains the least variance. Of interest is that the ENSO Non-canonical mode explains more variance if starting from 1945, while the opposite is true for the trend mode.

Of particular relevance to PDV are the results from A361. The two PDV modes are essentially unaltered with larger lag size used (6 month here and even 12 month in another test not shown). This suggests that the 1-yr time span (5 lags at 3-month intervals) used in the primary analysis, even if only intended to cover a significant portion of the ENSO evolution, is meanwhile sufficient to robustly characterize the temporal variability (i.e., PC time series) associated with the decadal modes. Now that the primary analysis gets the PCs right, the PDV spatial patterns at larger time intervals (e.g., 1 year) can be readily obtained using lead/lag regressions, which are, by definition, identical to the eigenvectors obtained in an extended EOF analysis using the same lag size and number of lags (see Section A.4 for the mathematical derivation). In short, pre-filtering and larger lag size are not necessary to obtain the essentially identical results for the PDV modes. With the ENSO and PDV modes robustly extracted in the primary analysis, the other modes, as a result, have greater chance to be so extracted as well.

Table 4.3. Results of the sensitivity tests. Column 1 shows the leading modes identified in the primary analysis, the two numbers in each row indicating the percentage variance explained by a mode and its rank, respectively. Columns 2–6 each show the leading modes identified in a sensitivity test, the slash-delimited numbers indicating the correlation coefficient between the principal components of a specific mode in the sensitivity test and the primary analysis, the percentage variance explained by that mode and its rank, in this order. Asterisks indicate "not applicable".

A351	A359	A350	A357	A353	A361
$ENSO^{+}$/17.7/1	1.00/16.6/1	1.00/18.4/1	1.00/16.6/1	0.99/17.2/1	*/ */*
$ENSO^{-}$/13.6/2	1.00/12.8/2	1.00/14.3/2	1.00/12.8/3	1.00/13.8/2	*/ */*
Trend/10.2/3	0.99/11.4/3	0.95/ 6.1/3	0.99/15.1/2	0.97/ 9.8/3	0.95/15.8/1
PDV^{PP}/ 5.3/4	0.99/ 5.0/4	0.82/ 4.1/6	1.00/ 4.9/4	−0.67/ 6.1/4	−0.88/ 6.7/2
$ENSO^{NC}$/ 4.3/5	0.98/ 3.8/6	0.97/ 6.0/4	1.00/ 4.1/5	0.84/ 3.5/6	*/ */*
PDV^{NP}/ 4.3/6	−0.99/ 4.4/5	−0.79/ 4.7/5	0.99/ 4.0/6	0.73/ 3.2/7	−0.93/ 6.0/3
Biennial/ 3.5/7	0.98/ 3.4/7	0.98/ 3.8/7	1.00/ 3.3/7	0.94/ 3.5/5	*/ */*

4.3 Summary and discussions

Using rotated extended EOF analysis, all non-seasonal low frequency SST variability in the Pan-Pacific area during 1900–2002 is investigated, with seven modes robustly extracted in a *single* step: two related to canonical ENSO ($ENSO^{-}$ and $ENSO^{+}$), one related to departures from canonical ENSO (ENSO Non-canonical), two related to PDV (PDV Pan-Pacific and PDV North Pacific), and two others characterizing the biennial variability and long-term trend, respectively. The EOF analysis is featured by (1) a Pan-Pacific analysis domain that includes both tropical Pacific and extratropical North Pacific, (2) an all-season analysis period, (3) no pre-filtering or detrending of the SST anomalies (unlike in many previous studies), (4) extended EOF that provides a one-year or longer time sequence of the SST spatial patterns (i.e., not just a "snapshot" of the mature phase patterns as in regular EOF, but also their *evolution* in time), and (5) VARIMAX rotation which enables simplified hence more describable and physically meaningful spatiotemporal structures. Without recourse to time filtering, PDV signals are—probably for the first time—nicely captured both spatially and temporally alongside that of ENSO in a *single* analysis. This shall definitely help to clarify and hopefully lead to a better understanding of the spatiotemporal structures of PDV in the context of ENSO variability (and other components of Pacific low-frequency variability as well). It meanwhile allows a direct intercomparison between the various modes; lead/lag correlations of which are often useful in diagnosing and modeling causes and effects in the Pacific ocean-atmosphere system. Specifically, current results show that

- a tropical interannual mode, termed ENSO Non-canonical, is present in the Pacific Ocean to account for the departures from canonical ENSO evolution. SST patterns associated with this mode is characterized by an eastward development of warmer-than-normal SSTs along the equator, which differs from a canonical depiction of ENSO evolution. The associated PC time series has greater amplitudes during the post-climate-shift period (1977-onward), indicative relevance to the anomalous El Niño events occurred during 1982–83 and/or 1997–98.

- PDV is manifested through two modes of quite different geographical emphasis and evolution characteristics. The Pan-Pacific mode is more of a "canonical" picture with positive SST anomalies in central North Pacific and negative SST anomalies to the north/south and along/off the U.S. west coast. Negative SST anomalies develop along the U.S. west coast to be stronger than -0.3°C in about 4 years, which leads the development of positive SST anomalies in central North Pacific. The North Pacific mode, as suggested by the name, is on the other hand essentially restricted to North Pacific during its mature phase, with same-signed SSTs across almost all the longitudes from east of Japan to off the U.S. west coast. Tropical signatures do exist, with development and decay of SST anomalies in equatorial eastern Pacific leading their counterpart in North Pacific by about 1 year. Climate shifts are evident in both the Pan-Pacific mode and the North Pacific mode, but not simultaneously. Specifically, the well documented regime shift occurred around 1976–77 is tracked by the North Pacific mode. The two modes are both evidenced biologically, to considerable extent.

- SST variability associated with ENSO does not *directly* link to that associated with PDV, and vice versa, as suggested by lead/lag correlations of the corresponding principal components. The PDV modes themselves are however interlinked, with the Pan-Pacific mode leading the North Pacific mode by about 44 years.

- the rotated extended EOF technique is able to robustly extract Pacific low frequency SST variability in a single step without recourse to time filtering. The extractions are stable to perturbations in analysis domain, analysis period, definition of climatology, number of modes rotated, lag size etc. The same technique has a promising application in future studies with newer data sets and/or variables.

Despite successful characterization of the various low-frequency modes in the Pan-Pacific area, current results definitely lack an insight of the underlying processes and mechanisms responsible for each. Conceivably, SST variations in the Pacific could be generated by wind-induced surface forcing and by subsurface dynamics as well. An immediate follow-up shall be an analysis of combined variability of SST and ocean heat content; the latter has already been shown by modeling studies to be instrumental in PDV dynamics. Simulations with ocean general circulation model (GCM) showed that significant decadal variability in SST could be found in the Kuroshio-Oyashio Extension (KOE) region, which is a "window" (open only in winter) area of surface-subsurface interactions (Xie et al. 2000). Using the production of a simple ocean data assimilation (Carton et al. 2000b,a), Tomita et al. (2002) diagnosed the relative importance of surface forcing and subsurface geostrophic advection in generating decadal SST variations; the latter was found to contribute significantly in the KOE region. Recent study by Hosoda et al. (2004) reassured the importance of subsurface dynamics in PDV simulation. That subsurface plays an important role in PDV suggests the latter to be potentially predictable as subsurface observations and simulations advance. Due to data unavailability or lack thereof, many low frequency studies lacks an insight of subsurface variables and processes. Annually resolved gridded world ocean heat content data has just become available at National Oceanographic Data Center for the period of 1955–2003 (Levitus et al. 2005), which well deserves exploration in the follow-up study.

Chapter 5

Work Schedule

The primary analysis (see Section 3.6.1.1), which is part of the proposed work, has already been conducted, with considerable success in PDV characterization. An immediate follow-up will be the extension of the primary analysis to other SST data sets, both observed and simulated. Ocean heat content will also be analyzed, either independently or in combination with SST. This will finish up the first part of the proposed work, i.e., PDV characterization. The second part of the work involves the analysis of PDV lead/lags and development of hypothesis on PDV mechanisms. I expect the whole work to be completed in about one and a half years from now, with the schedule as follows:

- Primary analysis of Pacific low-frequency SST variability (completed)
  - Rotated extended EOF
  - Sensitivity tests
- Analysis of other SST data sets (3 months)
  - Observed SST
  - IPCC's 20^{th} century climate simulations
  - Longer analysis period (1870-onward, for example)
- Analysis of PDV lead/lags for key oceanic and atmospheric variables (3 months)
  - Ocean heat content
  - Atmospheric reanalysis
  - Residual diagnosis of atmospheric diabatic heating
- Development/filtering of PDV mechanisms: diagnostic focus (3 months)
- Development/filtering of PDV mechanisms: modeling focus (3 months)
- Write up (3 months)

Total time proposed: 15 months

Appendix A

Rotated Extended EOF

A.1 Construction of data matrix

First, seasonal means of any variable are obtained by averaging over DJF, MAM, JJA and SON, which are then demeaned and deseasoned, denoted by

$$A(t) = \begin{bmatrix} a_{1,1} & a_{1,2} & \dots & a_{1,M} \\ a_{2,1} & a_{2,2} & \dots & a_{2,M} \\ \vdots & \vdots & \ddots & \vdots \\ a_{N,1} & a_{N,2} & \dots & a_{N,M} \end{bmatrix} \tag{A.1}$$

where N is the number of seasons, and M the number of grid cells. For extended EOF with $2L+1$ time lags of size Δt, a matrix A_E is constructed from A such that

$$A_E = \begin{bmatrix} A(t - L\Delta t) & A(t - (L-1)\Delta t) & \dots & A(t + L\Delta t) \end{bmatrix} \tag{A.2}$$

The matrix A_E is then normalized by the square root of spatially-integrated variance

$$\sigma = \sqrt{\sum_{n=1}^{N} \sum_{m=1}^{(2L+1)M} a_{n,m}^2 / N} \tag{A.3}$$

A.2 SVD-based EOF

Singular value decomposition (SVD) of A_E is given by

$$A_E = USV^T \tag{A.4}$$

where U and V satisfy

$$U^T U = I \tag{A.5}$$

$$V^T V = I \tag{A.6}$$

and S is a diagonal matrix containing the so-called singular values. The covariance matrix C can then be written as

$$C = A_E^T A_E / N = V(S^T S/N)V^T \tag{A.7}$$

Post-multiplying by V we get

$$CV = V(S^T S/N) \tag{A.8}$$

The above is a eigenvalue problem, of which the eigenvectors V and eigenvalues $S^T S/N$ can be obtained from Eqn. A.4. The modal decomposition of A_E can then be achieved by grouping U and S in Eqn. A.4 to form the time series corresponding to the eigenvectors. Alternatively, one can group S and V to form the spatial patterns (or EOFs), with U being the time series (hereafter principal components). The decomposition is thus

$$A_E = TX^T \tag{A.9}$$

where

$$T = U \tag{A.10}$$

and

$$X^T = SV^T \tag{A.11}$$

In practice, one may want to scale T and X by a factor of $\sqrt{N}$ such that the principal components have variance one. Note the units (if any) of A_E are now carried by the spatial patterns X, while the principal components T are dimensionless. The advantage of SVD-based EOF is that there is no need to construct the covariance matrix, and it requires fewer computational steps. In Matlab, SVD is achieved by the function of the same name.

A.3 VARIMAX rotation

Let R denote the rotation matrix, which satisfies

$$R^T R = I \tag{A.12}$$

The rotated EOFs and corresponding principal components are nothing but

$$X_R = XR \tag{A.13}$$

$$T_R = TR \tag{A.14}$$

Here we have

$$T_R X_R^T = TR(XR)^T = TRR^T X^T = TX^T \tag{A.15}$$

which, by comparison with Eqn. A.9, gives

$$A_E = T_R X_R^T \tag{A.16}$$

Thus, the matrix A_E can be recovered from the rotated EOFs to the extent they are included in the rotation. Further, the orthogonality of the principal components is maintained after

the rotation since

$$T_R^T T_R = (TR)^T TR = (UR)^T UR = R^T U^T UR = I \tag{A.17}$$

The orthogonality of the EOFs, however, are relaxed for the sake of simplified spatial structures since

$$X_R^T X_R = (XR)^T XR = (VS^T R)^T VS^T R = R^T SV^T VS^T R = R^T SS^T R \tag{A.18}$$

is not diagonal.

A.4 Lead/lag regressions

This section discusses the relationship between the spatial patterns X_R and lead/lag regressions of A on the principal components T_R. It can be easily shown that the results also hold for unrotated case.

Partitioning X_R into $2L+1$ submatrices, each of which containing M rows, we rewrite Eqn. A.16 as

$$A_E = T_R \begin{bmatrix} X_R(t-L\Delta t) \\ X_R(t-(L-1)\Delta t) \\ \vdots \\ X_R(t) \\ \vdots \\ X_R(t+(L-1)\Delta t) \\ X_R(t+L\Delta t) \end{bmatrix}^T \tag{A.19}$$

which, by comparison with Eqn. A.2, gives

$$A(t-l\Delta t) = T_R X_R^T(t-l\Delta t) \qquad (-L \leqslant l \leqslant L) \tag{A.20}$$

Let $\mathbf{t}_k$ denote the k^{th} column of T_R, $\mathbf{x}_k(t-l\Delta t)$ denote the k^{th} column of $X_R(t-l\Delta t)$, Eqn. A.20 can be rewritten as

$$A(t-l\Delta t) = \mathbf{t}_1\mathbf{x}_1^T(t-l\Delta t) + \mathbf{t}_2\mathbf{x}_2^T(t-l\Delta t) + \ldots + \mathbf{t}_K\mathbf{x}_K^T(t-l\Delta t) \tag{A.21}$$

where K is the number of EOFs included in the rotation. Using Eqn. A.21 and recalling Eqn. A.17, the regression of $A(t-l\Delta t)$ on $\mathbf{t}_k$ can be obtained as

$$\begin{aligned} \frac{\mathrm{COV}(A(t-l\Delta t), \mathbf{t}_k)}{\mathrm{VAR}(\mathbf{t}_k)} &= \frac{A^T(t-l\Delta t)\mathbf{t}_k/N}{1/N} \\ &= (\mathbf{x}_1(t-l\Delta t)\mathbf{t}_1^T + \mathbf{x}_2(t-l\Delta t)\mathbf{t}_2^T + \ldots + \mathbf{x}_K(t-l\Delta t)\mathbf{t}_K^T)\mathbf{t}_k \\ &= \mathbf{x}_k(t-l\Delta t)\mathbf{t}_k^T\mathbf{t}_k \\ &= \mathbf{x}_k(t-l\Delta t) \end{aligned} \tag{A.22}$$

This shows that in extended EOF, lag regressions of matrix A on the principal components

are identical to the corresponding spatial patterns at the same time lag.

Bibliography

Barlow, M., S. Nigam, and E. H. Berbery, 2001: ENSO, Pacific decadal variability, and U.S. summertime precipitation, drought, and stream flow. *J. Climate*, **14**, 2105–2127.

Barnett, T. P., 1991: The interaction of multiple time scales in the tropical climate system. *J. Climate*, **4**, 269–285.

Barnett, T. P., D. W. Pierce, M. Latif, D. Dommenget, and R. Saravanan, 1999a: Interdecadal interactions between the tropics and midlatitudes in the Pacific basin. *Geophys. Res. Lett.*, **26**, 615–618.

Barnett, T. P., D. W. Pierce, R. Saravanan, N. Schneider, D. Dommenget, and M. Latif, 1999b: Origins of the midlatitude Pacific decadal variability. *Geophys. Res. Lett.*, **26**, 1453–1456.

Carton, J. A., G. Chepurin, and X. Cao, 2000a: A simple ocean data assimilation analysis of the global upper ocean 1950–95. Part II: Results. *J. Phys. Oceanogr.*, **30**, 311–326.

Carton, J. A., G. Chepurin, X. Cao, and B. Giese, 2000b: A simple ocean data assimilation analysis of the global upper ocean 1950–95. Part I: Methodology. *J. Phys. Oceanogr.*, **30**, 294–309.

Chavez, F. P., J. Ryan, S. E. Lluch-Cota, and M. Ñiquen C., 2003: From anchovies to sardines and back: multidecadal change in the Pacific Ocean. *Science*, **299**, 217–221.

da Silva, A., C. Young, and S. Levitus, 1994: Atlas of Surface Marine Data 1994, Volume 1: Algorithms and Procedures. *NOAA Atlas NESDIS 6*, U.S. Department of Commerce, 83 pp.

Deser, C. and M. L. Blackmon, 1995: On the relationship between tropical and North Pacific sea surface temperature variations. *J. Climate*, **8**, 1677–1680.

Fletcher, J. O., R. J. Slutz, and S. D. Woodruff, 1983: Towards a comprehensive ocean-atmosphere dataset. *Trop. Ocean-Atmos. Newslett.*, **20**, 13–14.

Folland, C. K. and D. Parker, 1989: Observed variations of sea surface temperature. *Proc. NATO Advanced Research Workshop on Climate Ocean Interaction, Oxford, England*, Kluwer Academic Press.

Folland, C. K. and D. E. Parker, 1990: Observed variations of sea surface temperature. *Climate-Ocean Interaction*, M. E. Schlesinger, ed., Kluwer, 21–52.

— 1995: Correction of instrumental biases in historical sea surface temperature data. *Quart. J. Roy. Meteor. Soc.*, **121**, 319–367.

Frankignoul, C. and K. Hasselmann, 1977: Stochastic climate models, Part II: Application to sea-surface temperature variability and thermocline variability. *Tellus*, **29**, 289–305.

Gershunov, A. and T. P. Barnett, 1998: Interdecadal modulation of ENSO teleconnections. *Bull. Amer. Meteor. Soc.*, **79**, 2715–2725.

Gu, D. and S. G. H. Philander, 1997: Interdecadal climate fluctuations that depend on exchanges between the tropics and extratropics. *Science*, **275**, 805–807.

Hare, S. R. and N. J. Mantua, 2000: Empirical evidence for North Pacific regime shifts in 1977 and 1989. *Prog. Oceanogr.*, **47**, 103–145.

Hasselmann, K., 1976: Stochastic climate models, I. Theory. *Tellus*, **28**, 473–485.

Hosoda, S., S.-P. Xie, K. Takeuchi, and M. Nonaka, 2004: Interdecadal temperature variations in the North Pacific central mode water simulated by an OGCM. *J. Oceanogr.*, **60**, 865–877.

Jacobs, G. A., H. E. Hurlburt, J. C. Kindle, E. J. Metzer, J. L. Mitchell, W. J. Teague, and A. J. Walcraft, 1994: Decade-scale trans-Pacific propagation and warming effects of an El Niño. *Nature*, **370**, 360–363.

Kalnay, E. et al., 1996: The NCEP/NCAR 40-year reanalysis project. *Bull. Amer. Meteor. Soc.*, **77**, 437–471.

Kaplan, A., M. A. Cane, Y. Kushnir, A. C. Clement, M. B. Blumenthal, and B. Rajagopalan, 1998: Analysis of global sea surface temperatures 1856–1991. *J. Geophys. Res.*, **103**, 18567–18589.

Latif, M. and T. P. Barnett, 1994: Causes of decadal climate variability over the North Pacific and North America. *Science*, **266**, 634–637.

— 1996: Decadal climate variability over the North Pacific and North America: Dynamics and predictability. *J. Climate*, **9**, 2407–2423.

Lau, N.-C. and M. J. Nath, 1994: A modeling study of the relative roles of tropical and extratropical SST anomalies in the variability of the global atmosphere-ocean system. *J. Climate*, **7**, 1184–1207.

Levitus, S., J. Antonov, and T. Boyer, 2005: Warming of the world ocean, 1955–2003. *Geophys. Res. Lett.*, **32**, L02604, doi:10.1029/2004GL021592.

Liu, Z., S. G. H. Philander, and R. Pacanowski, 1994: A GCM study of tropical-subtropical upper-ocean mass exchange. *J. Phys. Oceanogr.*, **24**, 2606–2623.

Mantua, N. J. et al., 1997: A Pacific interdecadal climate oscillation with impacts on salmon production. *Bull. Amer. Meteor. Soc.*, **78**, 1069–1079.

Miller, A. J., D. C. Cayan, T. P. Barnett, N. E. Graham, and J. M. Oberhuber, 1994: Interdecadal variability of the Pacific Ocean: Model response to observed heat flux and wind stress anomalies. *Climate Dyn.*, **9**, 287–302.

Minobe, S., 1997: A 50–70 year climatic oscillation over the North Pacific and North America. *Geophys. Res. Lett.*, **24**, 683–686.

— 1999: Resonance in bidecadal and pentadecadal climate oscillations over the North Pacific: Role in climatic regime shifts. *Geophys. Res. Lett.*, **26**, 855–858.

Monahan, 2001: Nonlinear principal component analysis: Tropical Indo-Pacific sea surface temperature and sea level pressure. *J. Climate*, **14**, 219–233.

Nakamura, H., G. Lin, and T. Yamagata, 1997: Decadal climate variability in the North Pacific during the recent decades. *Bull. Amer. Meteor. Soc.*, **78**, 2215–2225.

Nigam, S. and C. Chung, 2000: ENSO surface winds in CCM3 simulation: Diagnosis of errors. *J. Climate*, **13**, 3172–3185.

Nitta, T. and S. Yamada, 1989: Recent warming of tropical sea surface temperature and its relationship to the Northern Hemisphere circulation. *J. Meteor. Soc. Japan*, **67**, 375–383.

Pierce, D. W., T. P. Barnett, and M. Latif, 2000: Connections between the Pacific Ocean

tropics and midlatitudes on decadal timescales. *J. Climate*, **13**, 1173–1194.

Rayner, N. A. et al., 2003: Global analyses of sea surface temperature, sea ice, and night marine air temperature since the late nineteenth century. *J. Geophys. Res.*, **108**, No. D14, 4407, doi:10.1029/2002JD002670.

Richman, M. B., 1986: Rotation of principal components. *Int'l J. Climatol.*, **6**, 293–335.

Tomita, T., S.-P. Xie, and M. Nonaka, 2002: Estimates of surface and subsurface forcing for decadal sea surface temperature variability in the mid-latitude North Pacific. *J. Meteor. Soc. Japan*, **80**, 1289–1300.

Trenberth, K. E., 1990: Recent observed interdecadal climate changes in the Northern Hemisphere. *Bull. Amer. Meteor. Soc.*, **71**, 988–993.

Trenberth, K. E. and J. W. Hurrell, 1994: Decadal atmosphere-ocean variations in the Pacific. *Climate Dyn.*, **9**, 303–319.

Vimont, D. J., J. M. Wallace, and D. S. Battisti, 2003: The seasonal footprinting mechanism in the Pacific: Implications for ENSO. *J. Climate*, **16**, 2668–2675.

Wallace, J. M. and D. S. Gutzler, 1981: Teleconnections in the geopotential height field during the Northern Hemisphere winter. *Mon. Wea. Rev.*, **109**, 784–812.

Wu, L., Z. Liu, R. Gallimore, R. Jacob, D. Lee, and Y. Zhong, 2003: Pacific decadal variability: The tropical Pacific mode and the North Pacific mode. *J. Climate*, **16**, 1101–1120.

Xie, S.-P., T. Kunitani, A. Kubokawa, M. Nonaka, and S. Hosoda, 2000: Interdecadal thermocline variability in the orth acific for 1958–1997: A GCM simulation. *J. Phys. Oceanogr.*, **30**, 2798–2813.

Zhang, Y., J. M. Wallace, and D. S. Battisti, 1997: ENSO-like interdecadal variability: 1900–93. *J. Climate*, **10**, 1004–1020.

Zhang, Y., J. M. Wallace, and N. Iwasaka, 1996: Is climate variability over the North Pacific a linear response to ENSO? *J. Climate*, **9**, 1468–1478.